

LIST OF FIGURES

Figure No.		Page No.
1	Site Plan	58
2	Plan of the Landslide	59
3	Geology of the Landslide Site as Shown on Part of the Hong Kong Geological Survey Sheet 7 (Sha Tin, 1:20 000-scale; GCO, 1986)	60
4	Topographic Map (September 1976)	61
5	Locations of Pre-1997 Ground Investigation Works and Landslid Incidents	62
6	Pre-1997 Ground Investigation Works in the Adjacent Areas	63
7	Sequence of Events on 2 July 1997	64
8	1997 Topographic Survey and Locations of Ground Investigation Works	65
9	Development of the Landslide (1978-1980)	66
10	Development of the Landslide (1980-1996)	67
11	Development of the Landslide (1980-1997 and 1996-1997)	68
12	Aerial Photograph Interpretation of Area Surrounding Lai Ping Road Landslide Site Prior to Its Development Based on Aerial Photographs Dated 16 December 1964	69
13	Field Measured Permeability	70
14	Piezometer Reading Records	71
15	Observed Minimum Groundwater Level in Saprolite	72
16	Observed Maximum Groundwater Level in Saprolite	73
17	Rainfall Records of GEO Raingauge No. N09 in June and July 1997	74

Figure No.		Page No.
18	Rainfall Isohyets for 24-hour Duration on 2 July 1997 (Ending 0:00 hours 3 July 1997)	75
19	Maximum Rolling Rainfall at Raingauge No. N09 and at Autographic Raingauge No. 151 at the Chinese University	76
20	Comparison of Rainfall Data Recorded at Raingauge No. N09 with Other Raingauges for Major Landslide Events	77
21	Return Period of the Maximum Rainfall Recorded at Raingauge No. N09	78
22	Monthly Maximum 24-hour Rainfall at the Chinese University Between July 1973 and July 1997	79
23	Sensitivity of Shear Strength on Slip Surfaces and Depth of Groundwater Table on Slope Stability	80
24	Finite Element Mesh for Seepage Analyses	81
25	Changes of Phreatic Surface Calculated by Seepage Analyses	82
26	Temporal Variation of Factor of Safety of Slip Surfaces 1 to 4 - Model 1	83
27	Temporal Variation of Factor of Safety of Slip Surfaces 1 to 4 - Model 2	84
28	Finite Difference Grid for Cross-Section 6-6'	85
29	Shear Strain Mobilisation During the Development of the Landslide Mechanism - Finite Difference Analysis	86
30	Dynamic Analysis of Mobility of Landslide Debris from Scar No. 1	87
31	Dynamic Analysis of Mobility of Landslide Debris from Scar No. 4	88

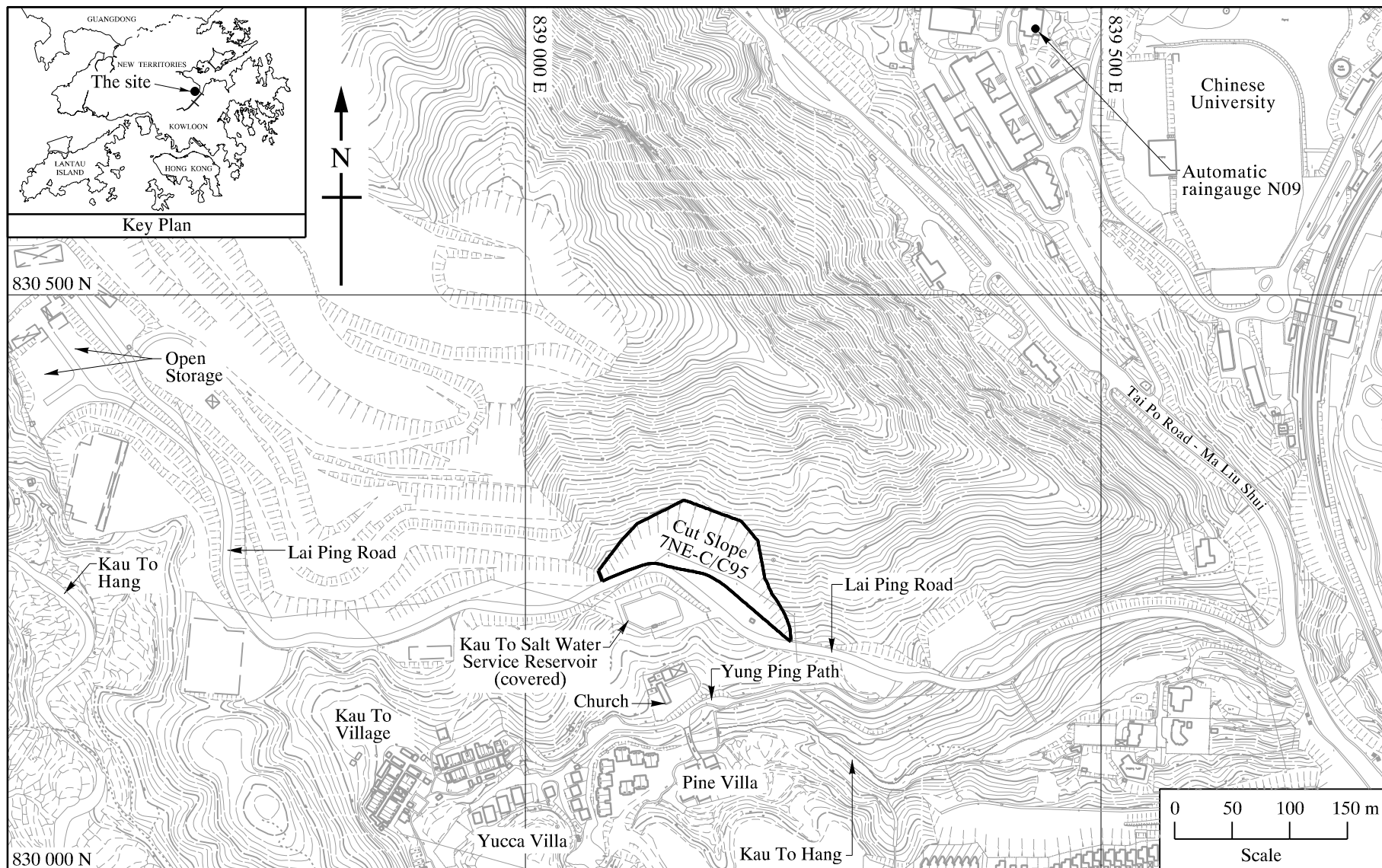


Figure 1 - Site Plan

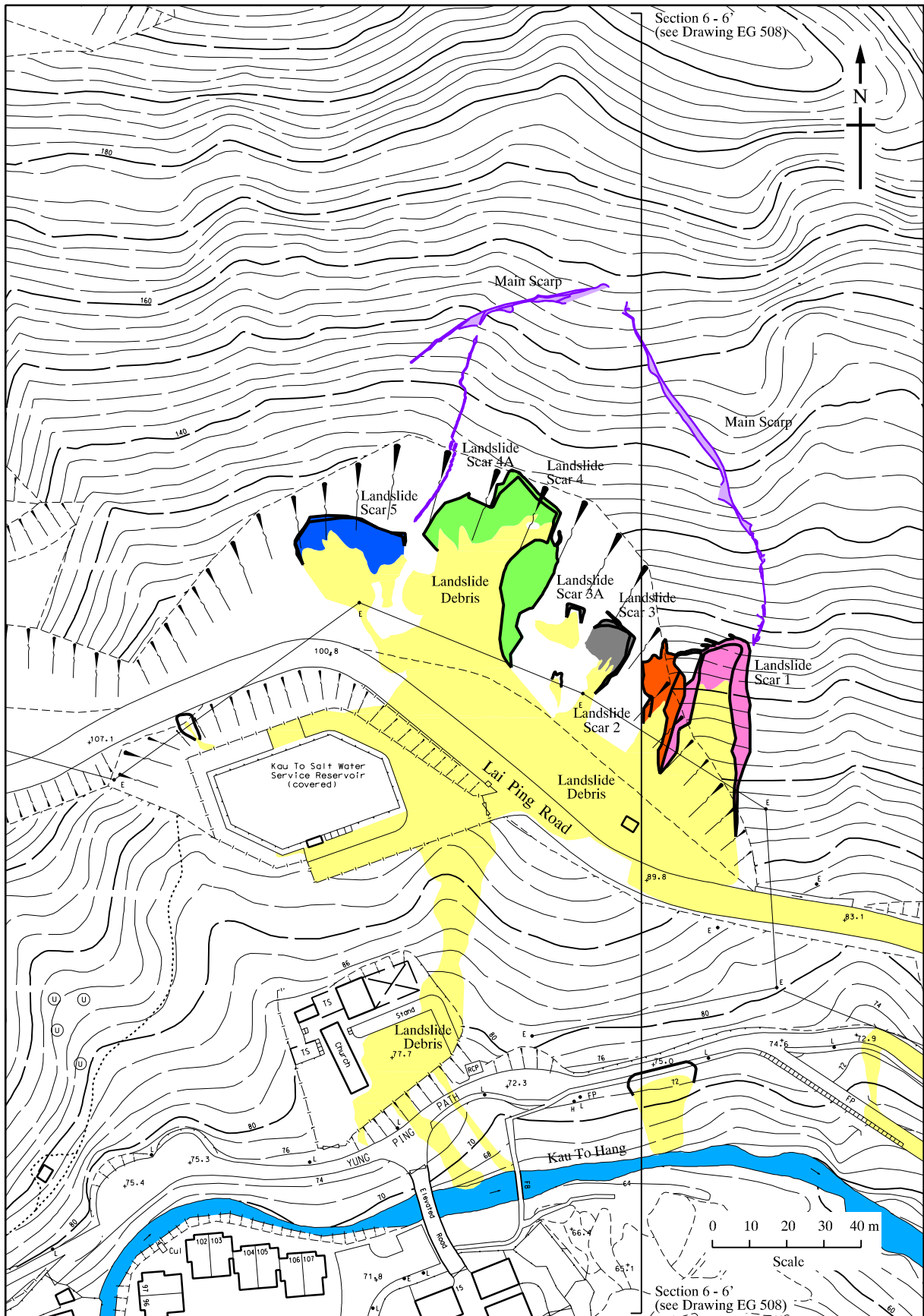


Figure 2 - Plan of the Landslide

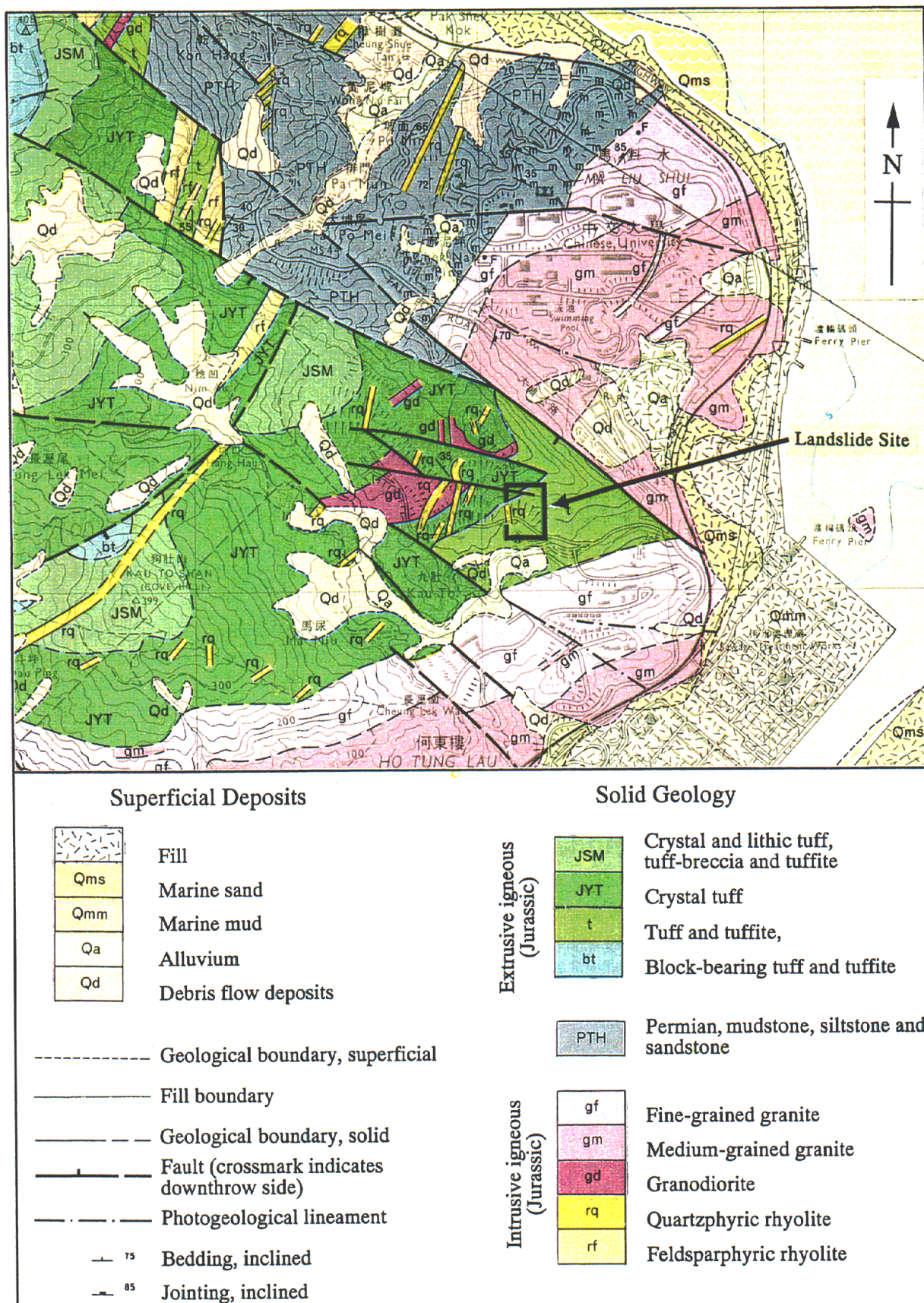


Figure 3 - Geology of the Landslide Site as Shown on Part of the Hong Kong Geological Survey Sheet 7 (Sha Tin, 1:20 000-scale; GCO, 1986)

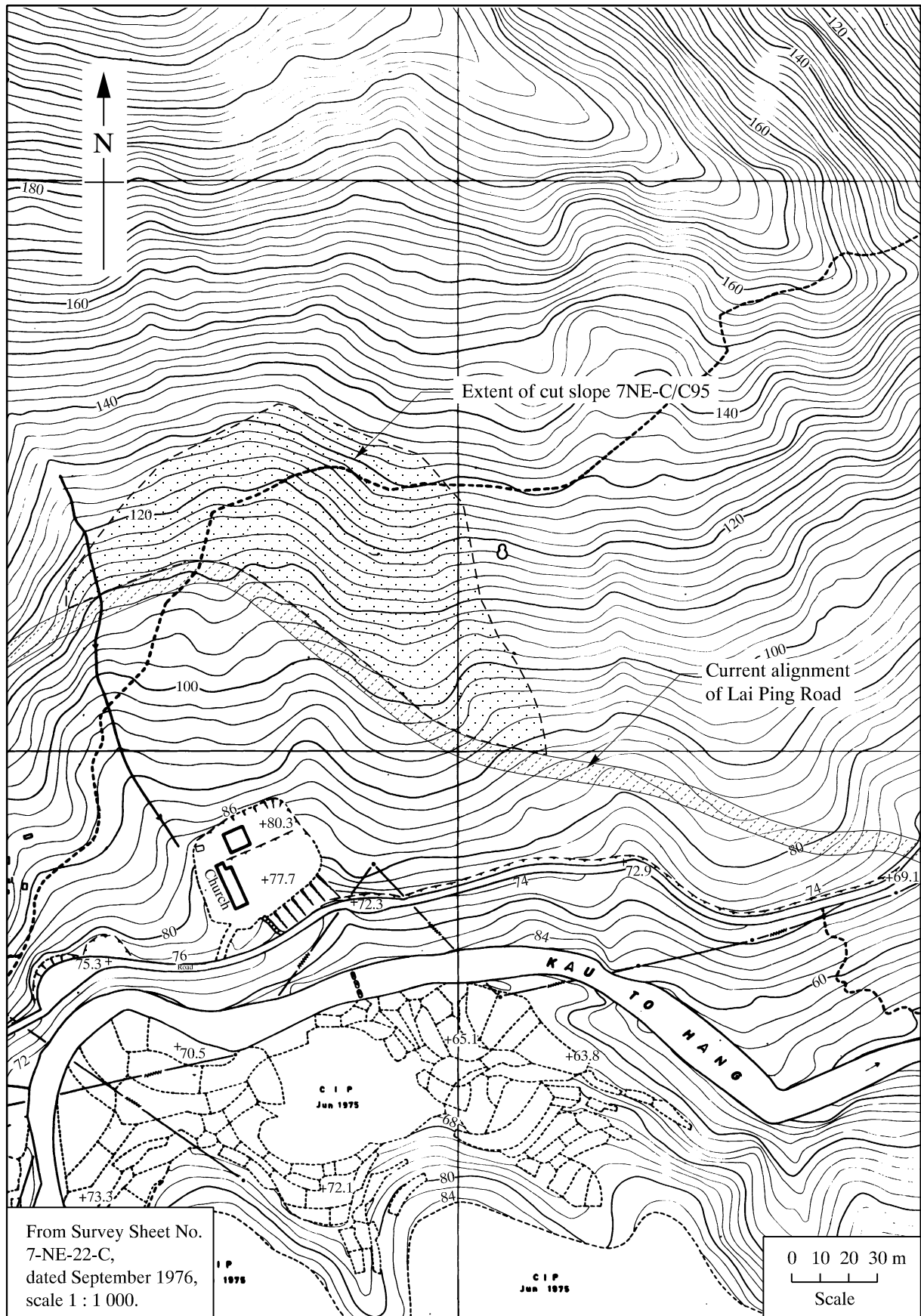


Figure 4 - Topographic Map (September 1976)

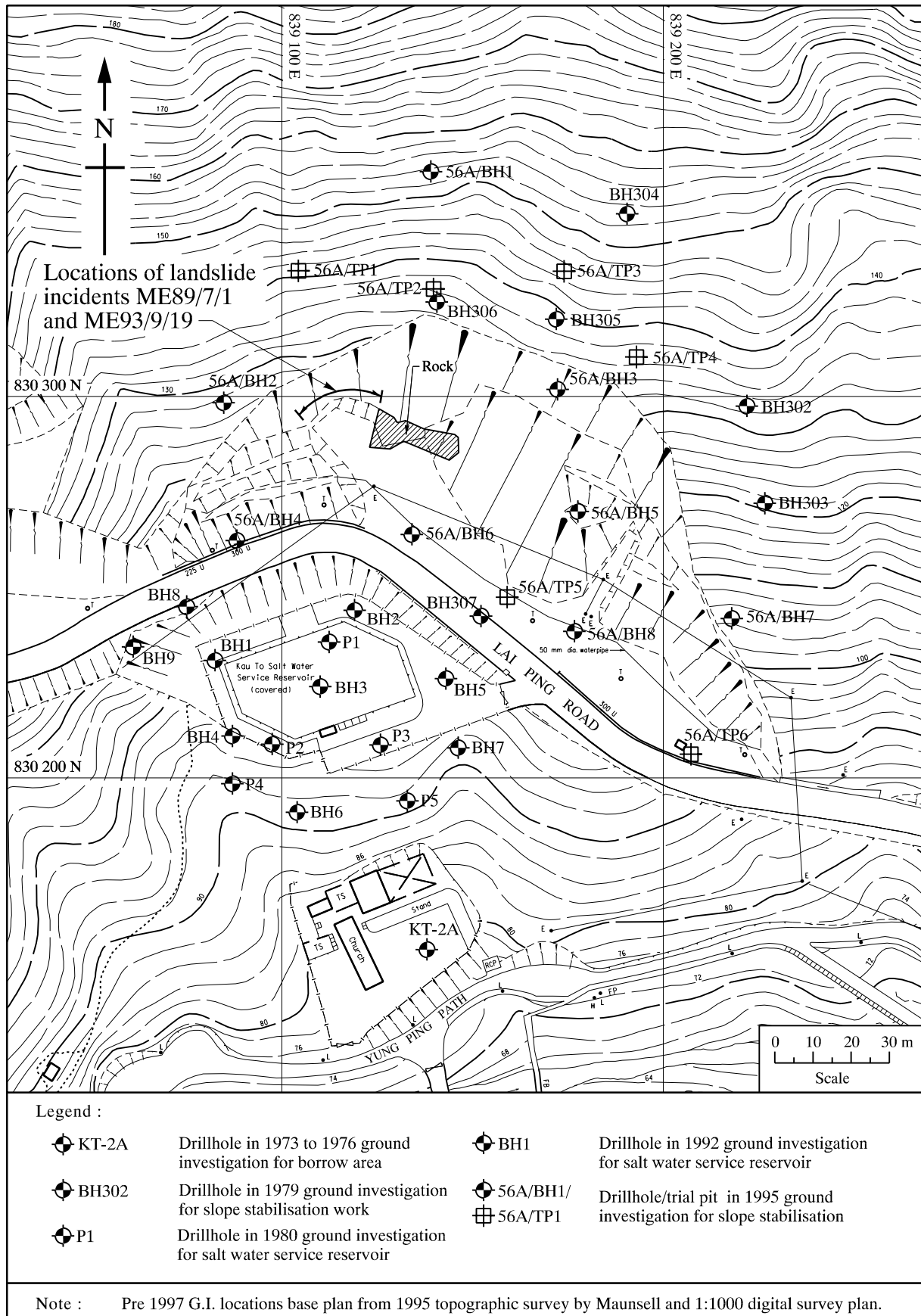


Figure 5 - Locations of Pre-1997 Ground Investigation Works and Landslide Incidents

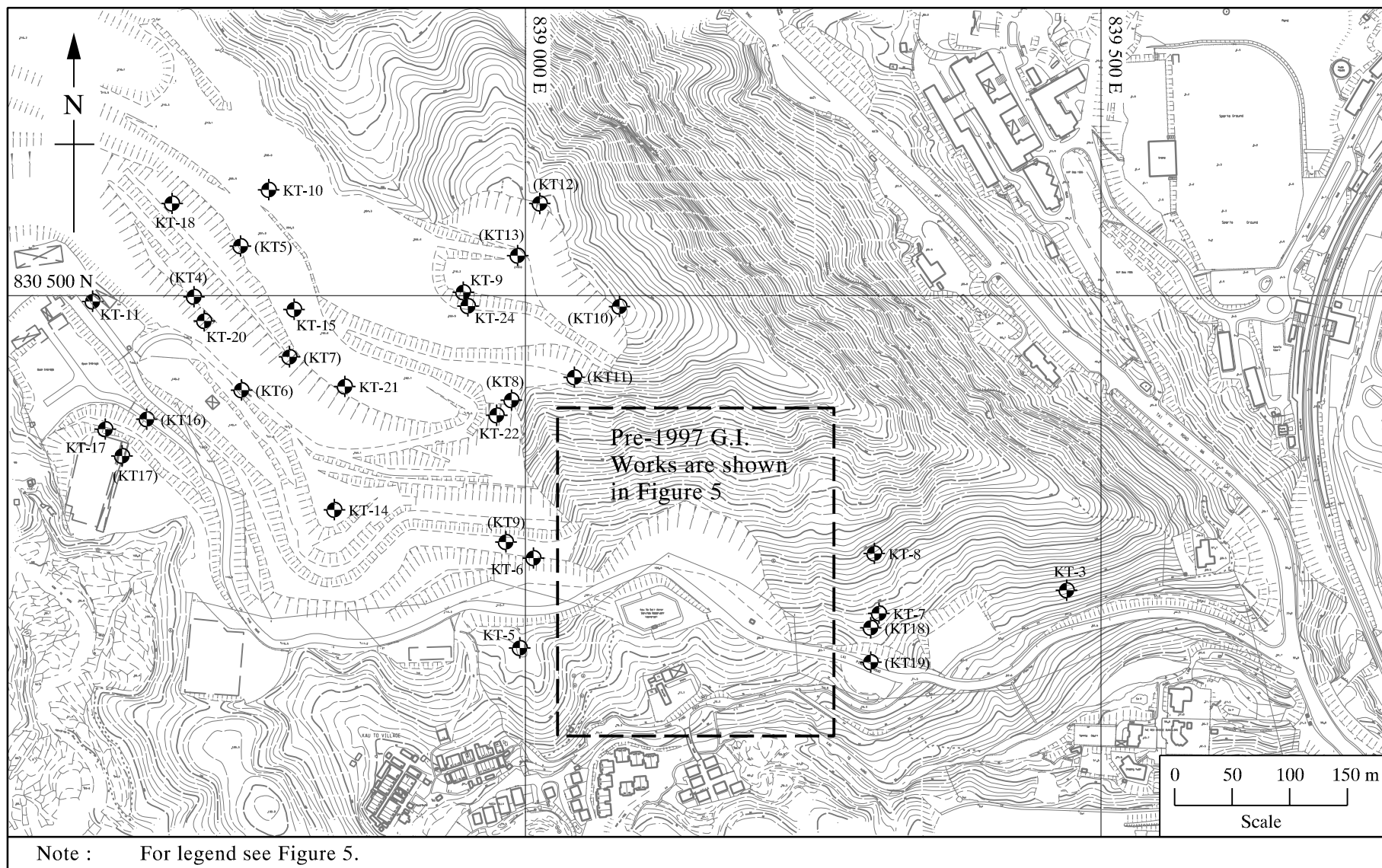


Figure 6 - Pre-1997 Ground Investigation Works in the Adjacent Areas

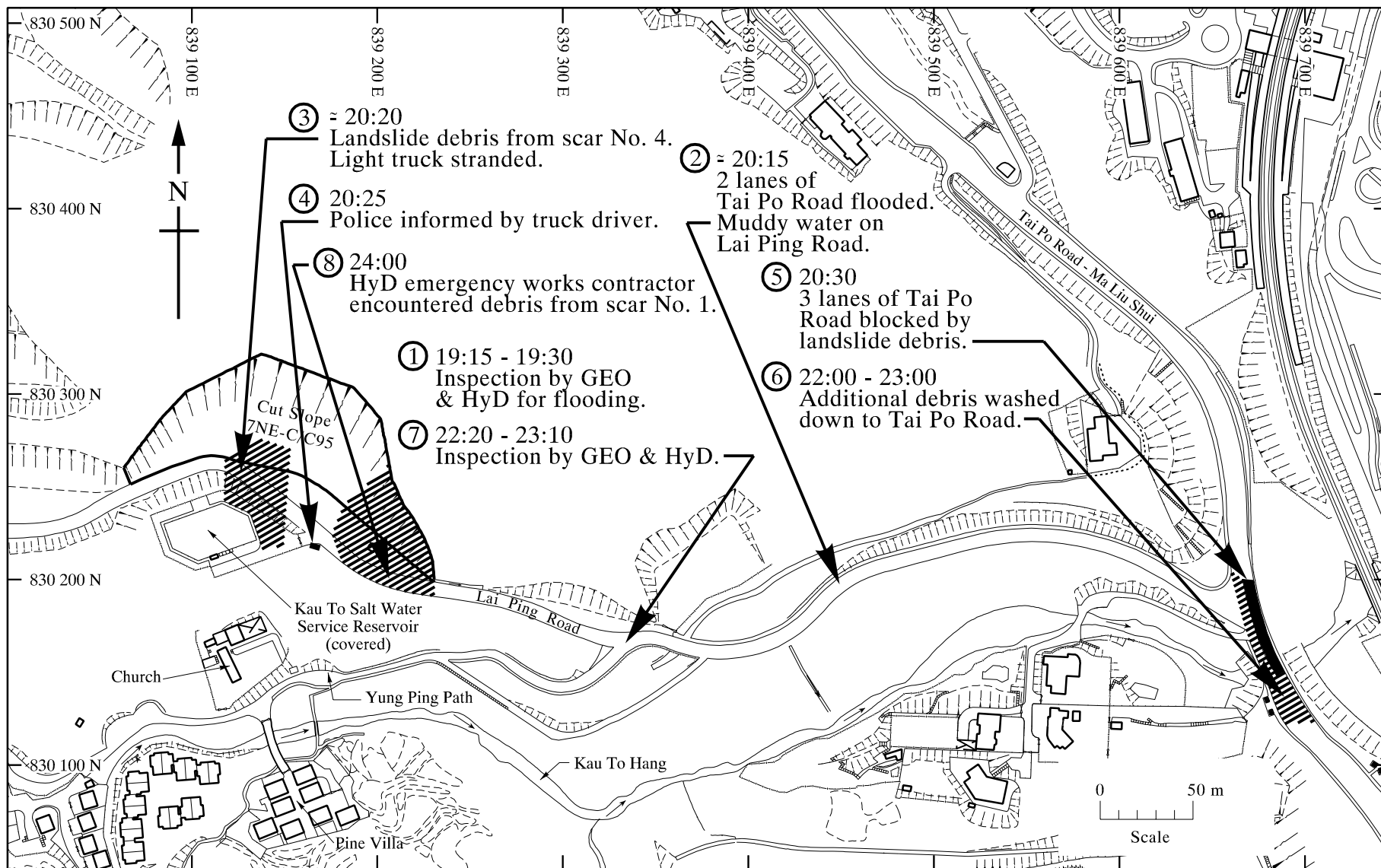


Figure 7 - Sequence of Events on 2 July 1997

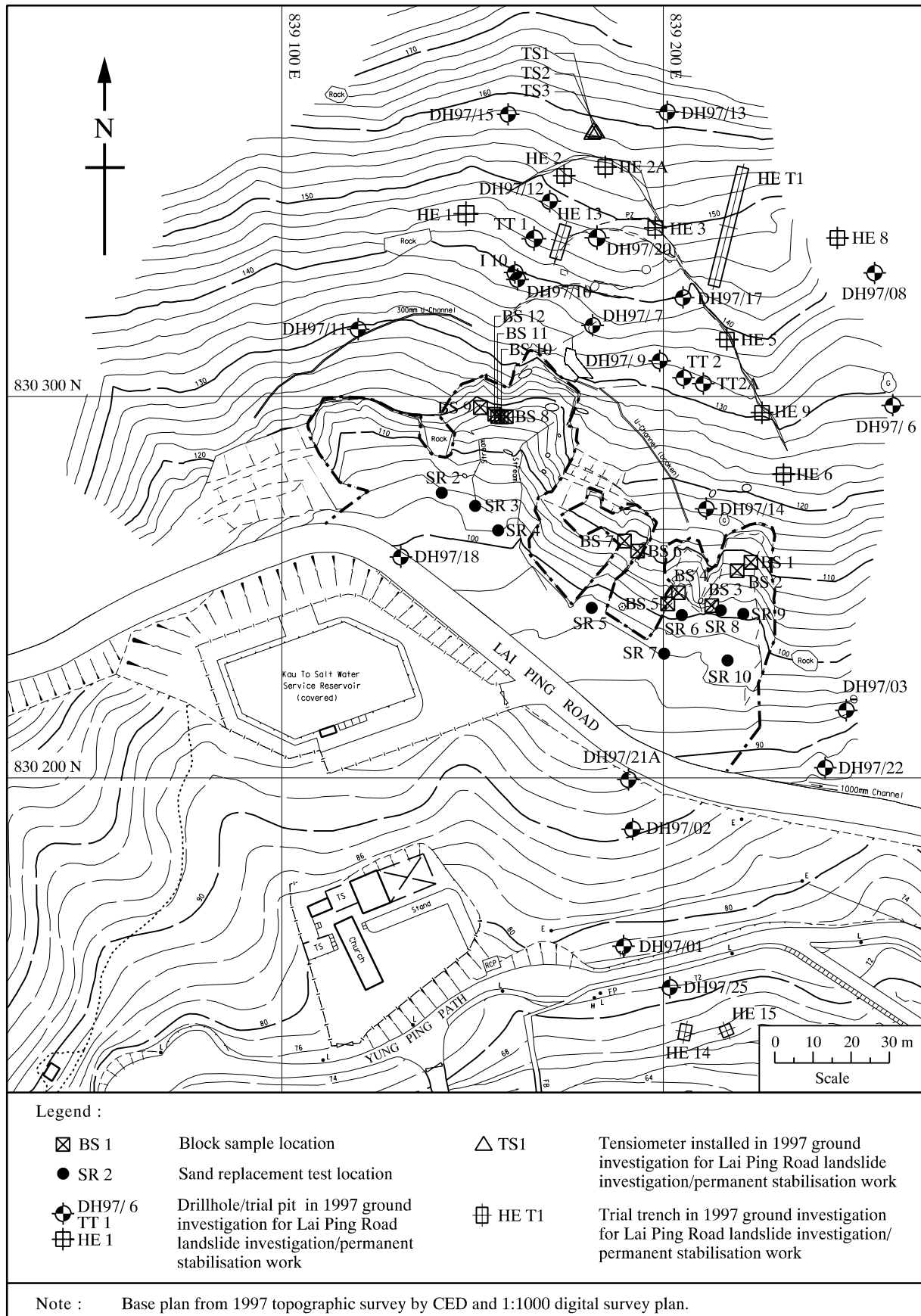


Figure 8 - 1997 Topographic Survey and Locations of Ground Investigation Works

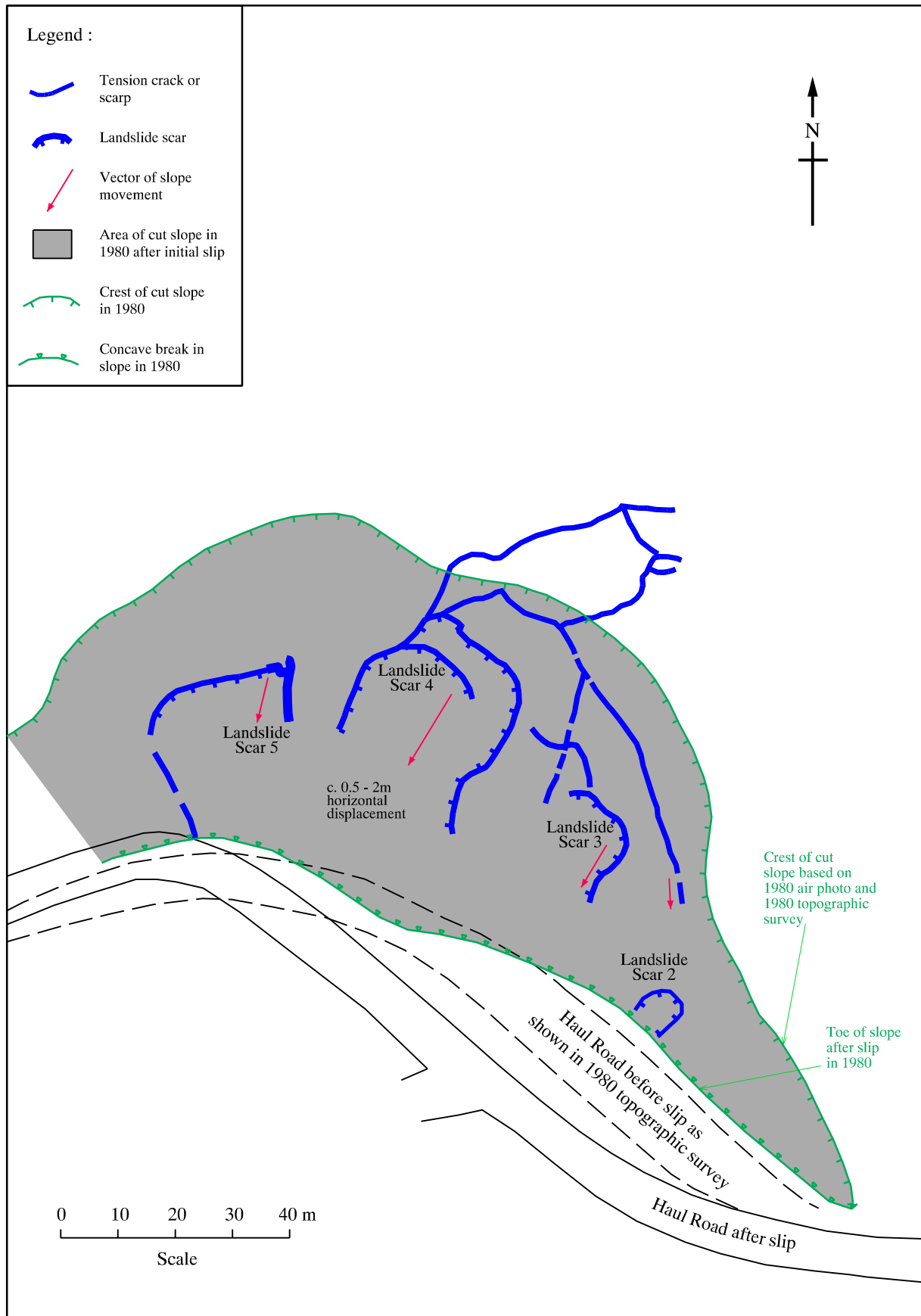


Figure 9 - Development of the Landslide (1978-1980)

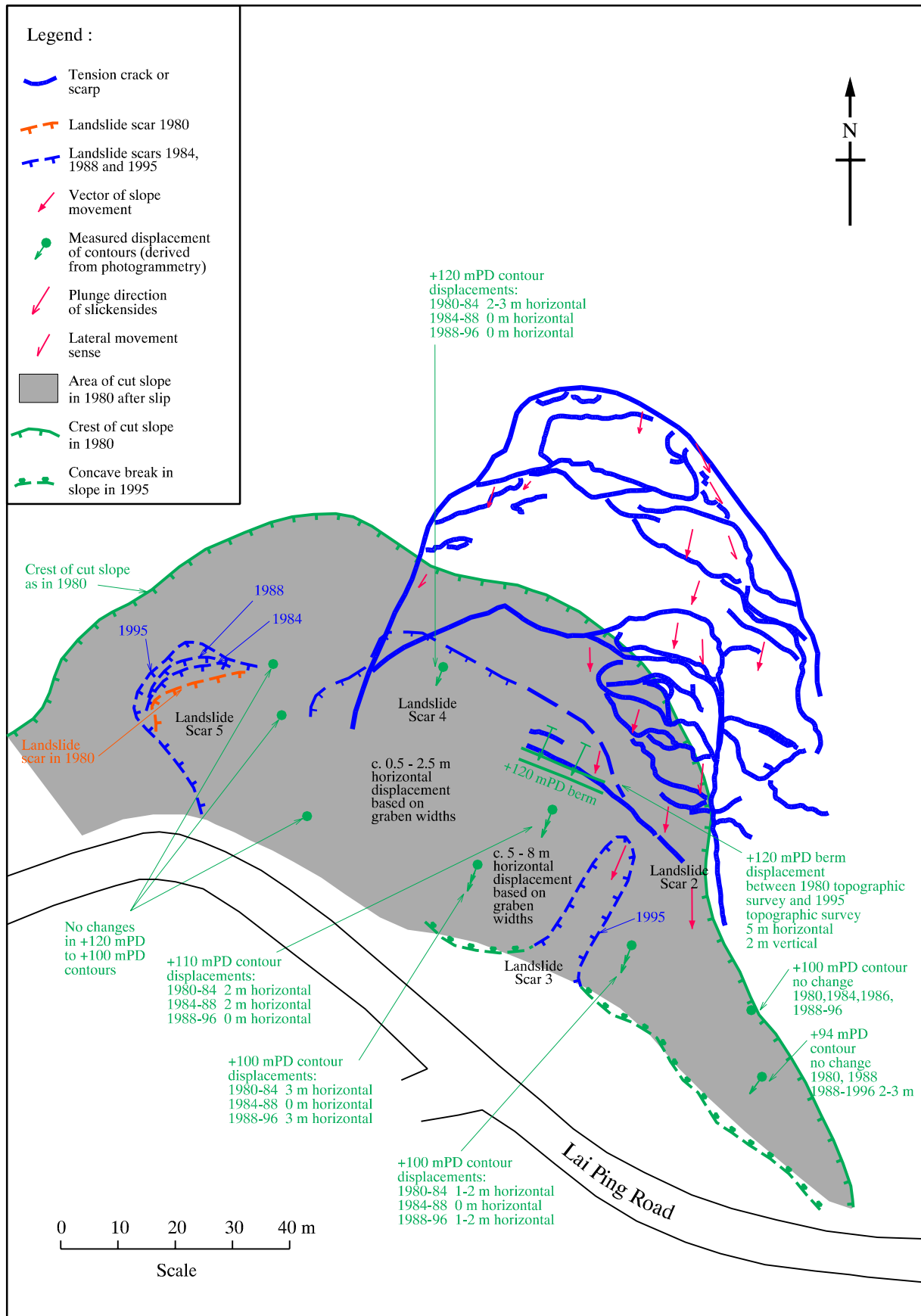


Figure 10 - Development of the Landslide (1980-1996)

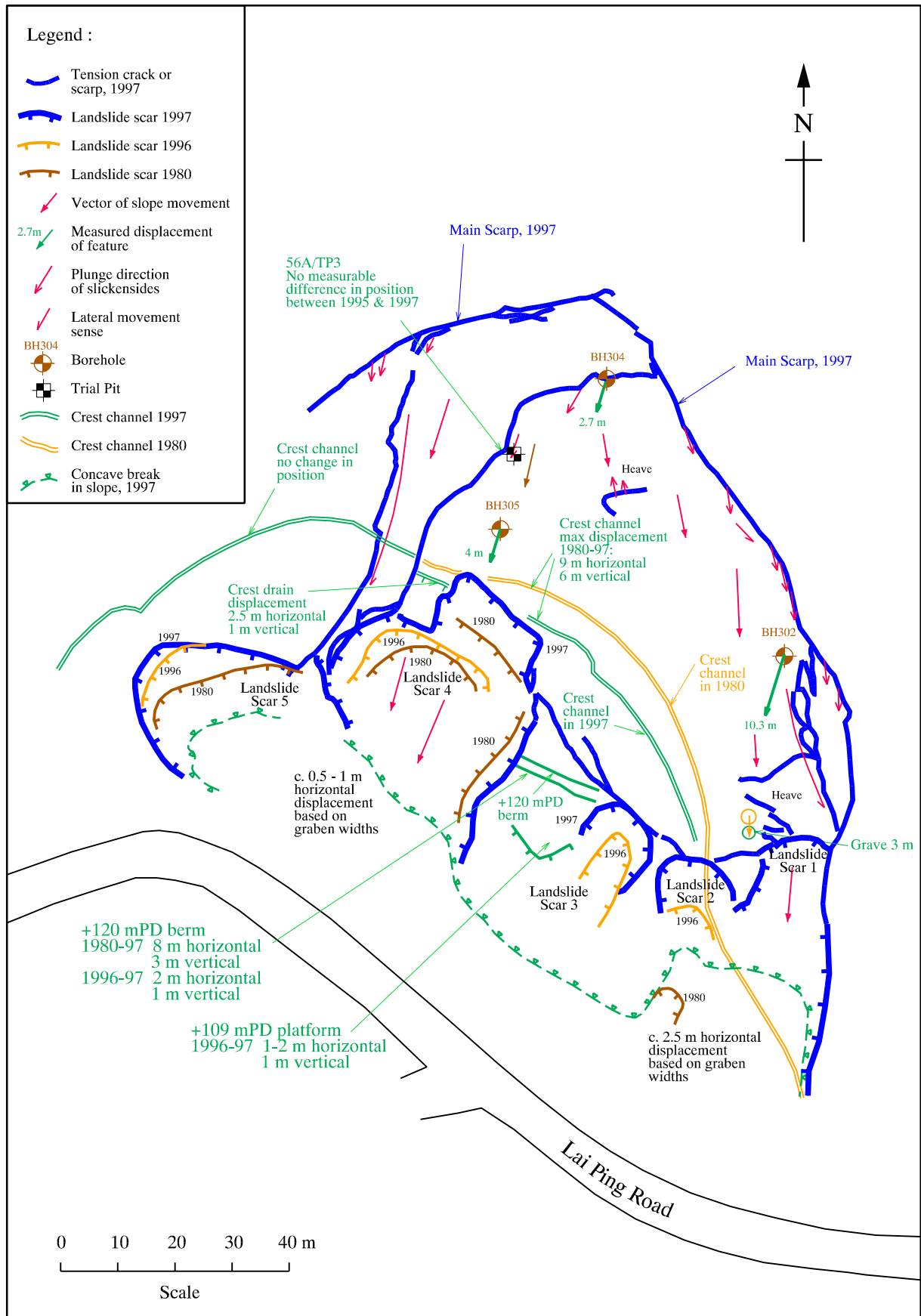


Figure 11 - Development of the Landslide (1980-1997 and 1996-1997)

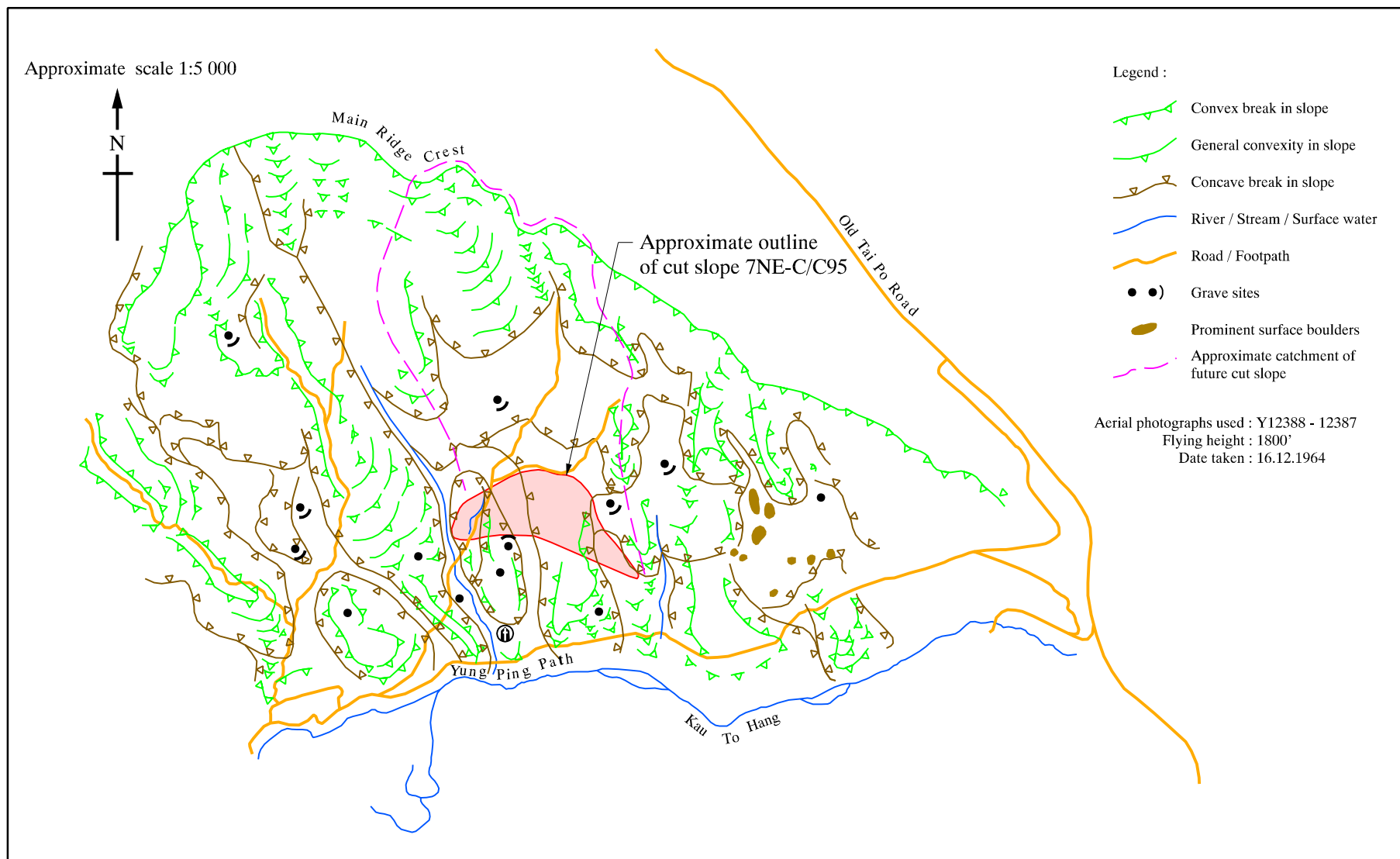
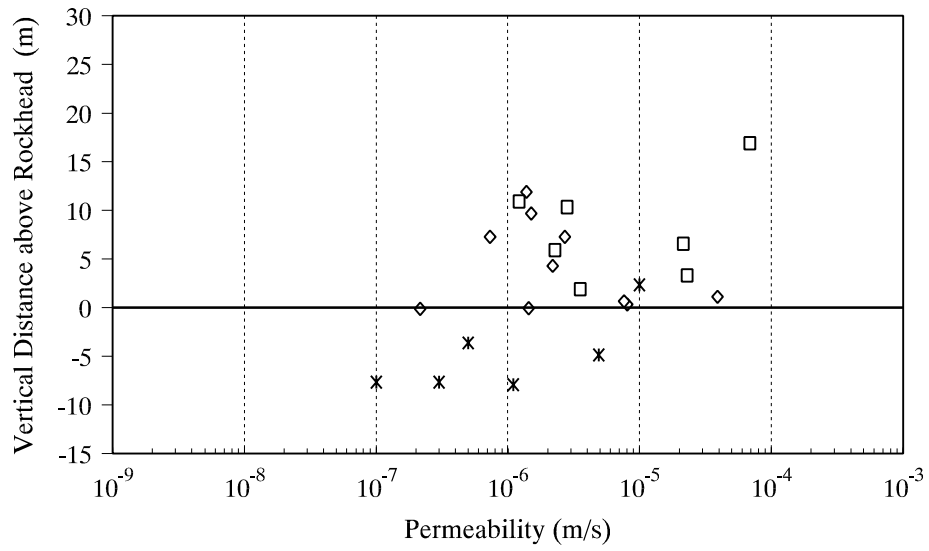
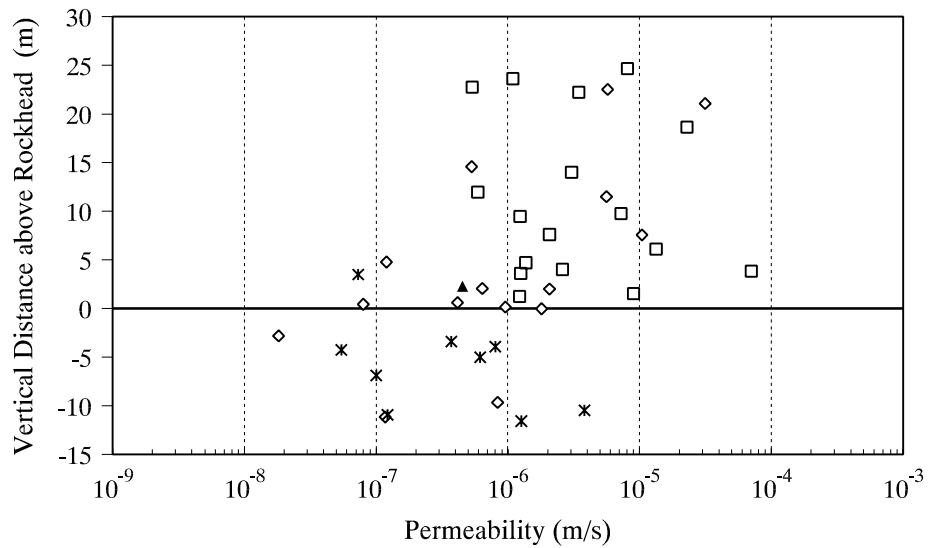


Figure 12 - Aerial Photograph Interpretation of Area Surrounding Lai Ping Road Landslide Site Prior to Its Development Based on Aerial Photographs Dated 16 December 1964



(a) Tests within the Slip Area



(b) Tests outside the Slip Area

Legend :

◇ Response test

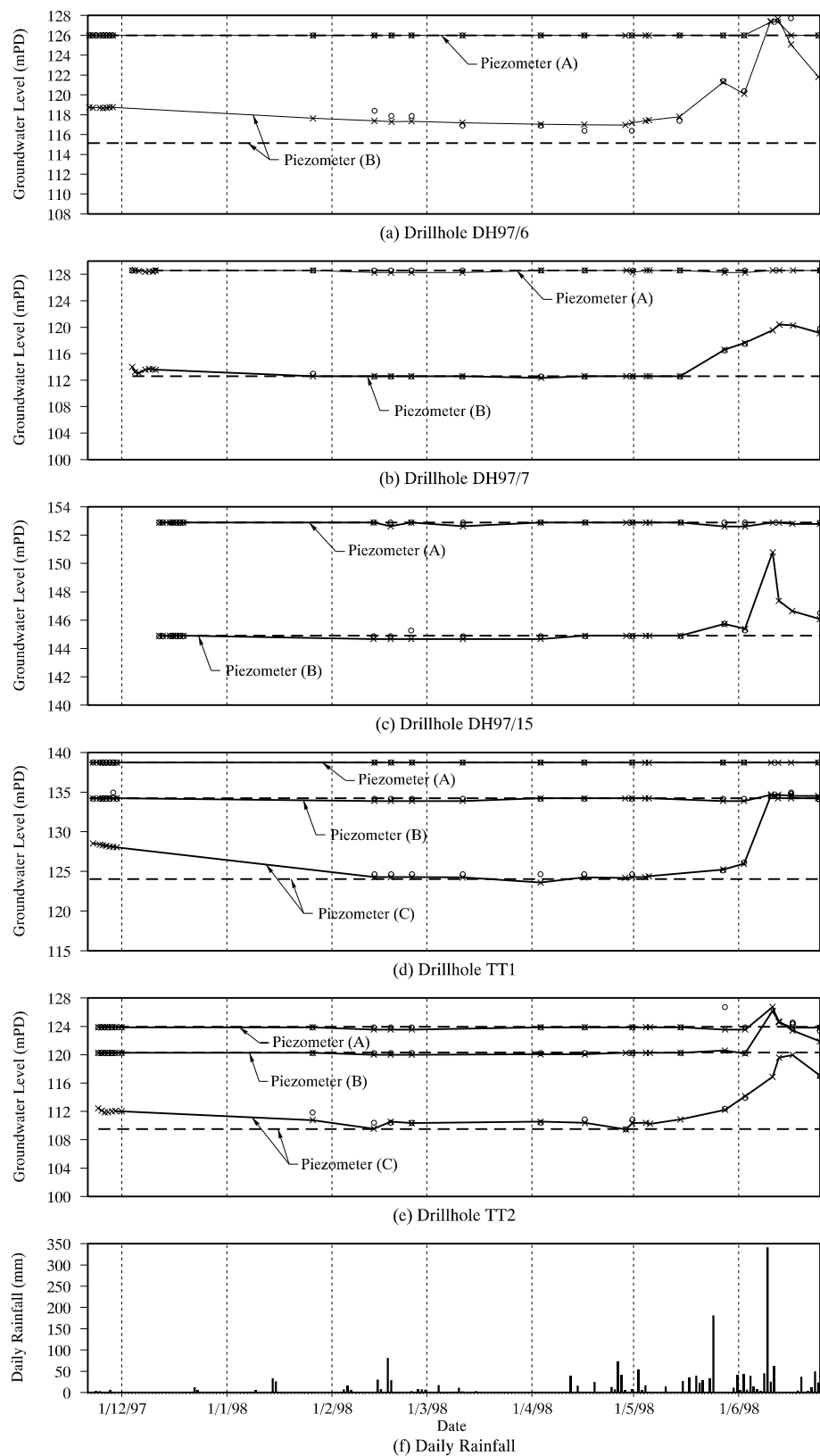
▲ Falling head test

□ Constant head test

× Packer test

Note : Rockhead is the top surface of the continuous or near-continuous moderately to slightly decomposed tuff in the PW 90/100 rock mass.

Figure 13 - Field Measured Permeability



Legend :

—x— Dip meter reading

○ Bucket reading

--- Level of piezometer tip

Figure 14 - Piezometer Reading Records

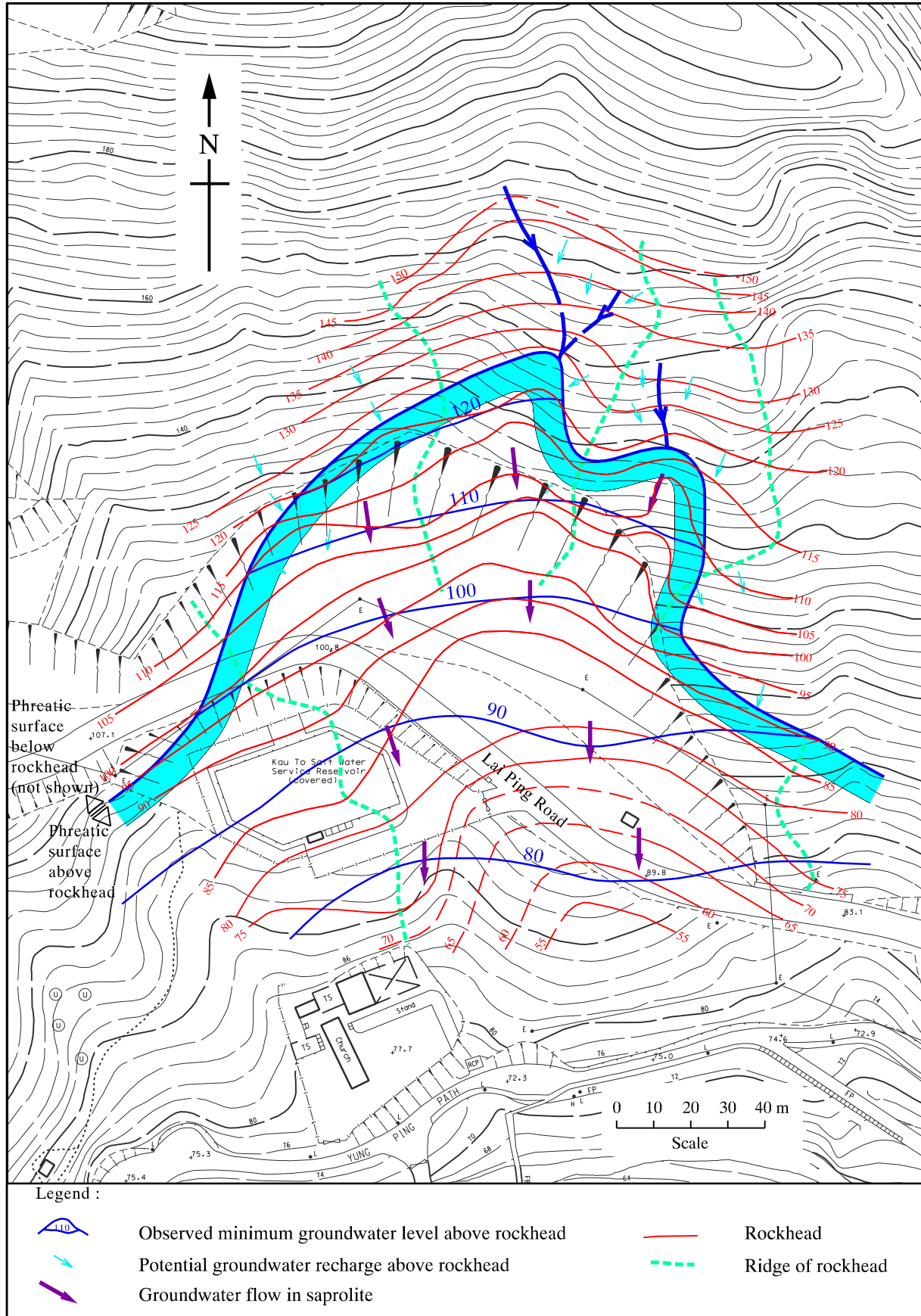


Figure 15 - Observed Minimum Groundwater Level in Saprolite

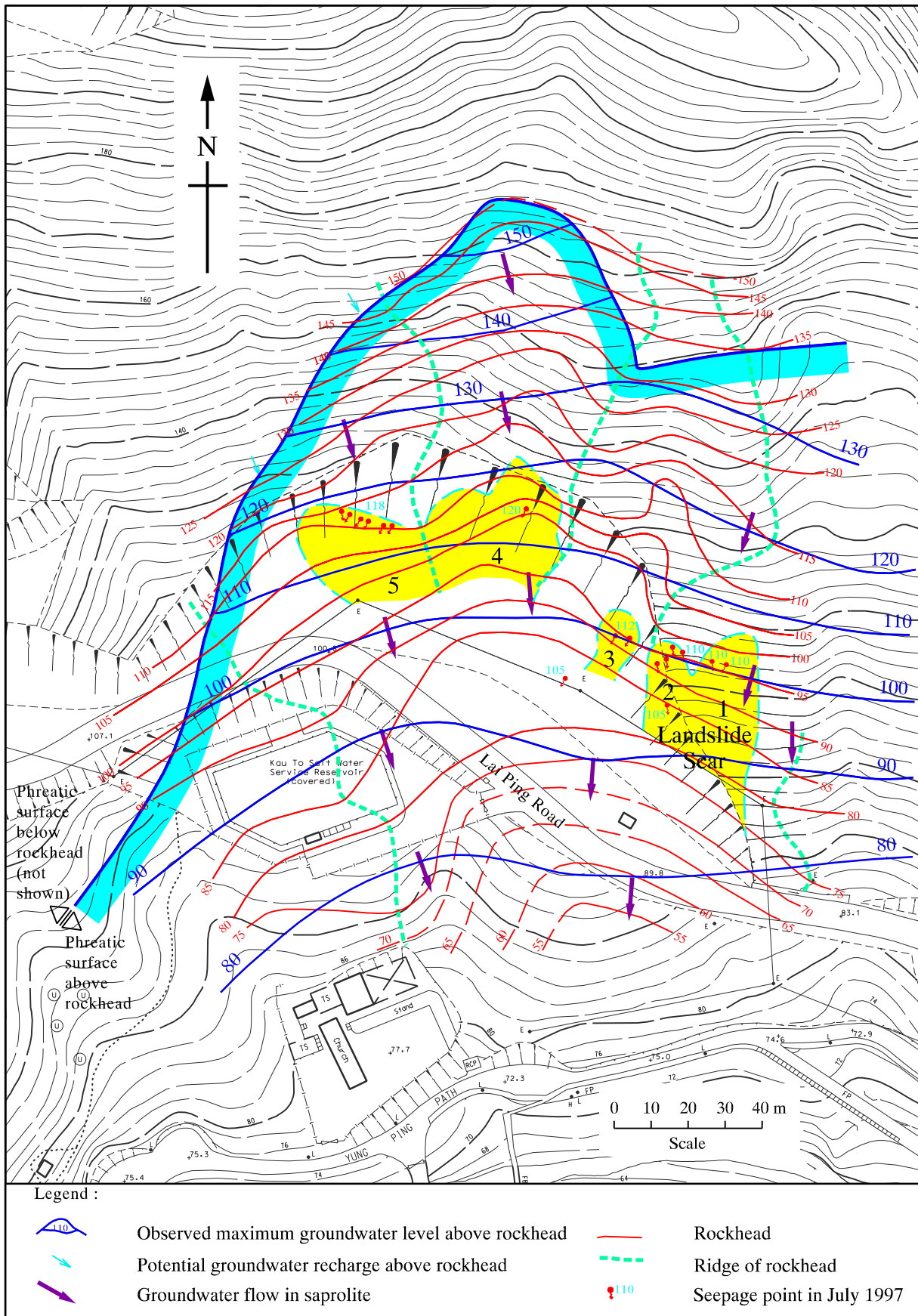


Figure 16 - Observed Maximum Groundwater Level in Saprolite

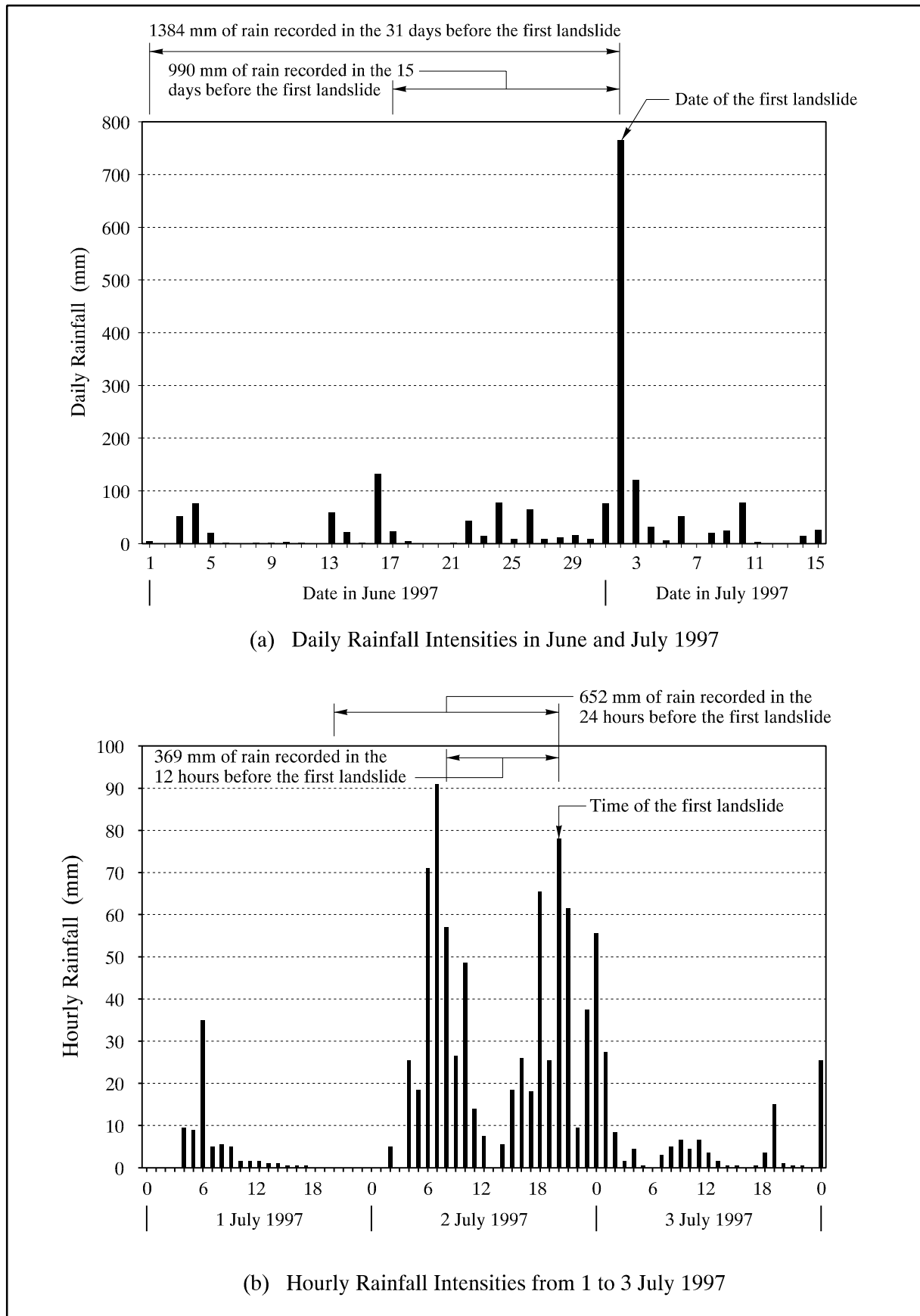


Figure 17 - Rainfall Records of GEO Raingauge No. N09 in June and July 1997

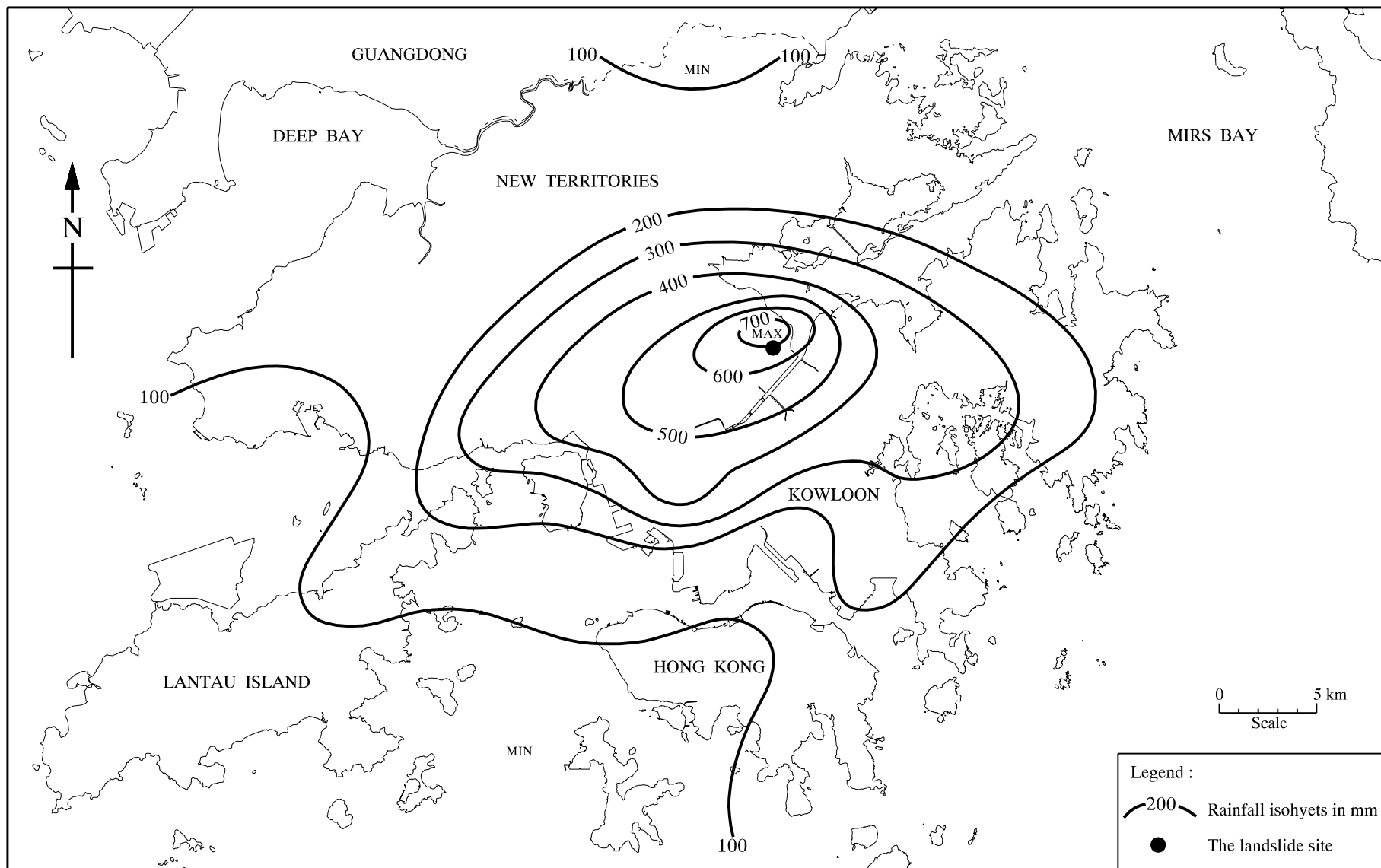


Figure 18 - Rainfall Isohyets for 24-hour Duration on 2 July 1997 (Ending 0:00 hours 3 July 1997)

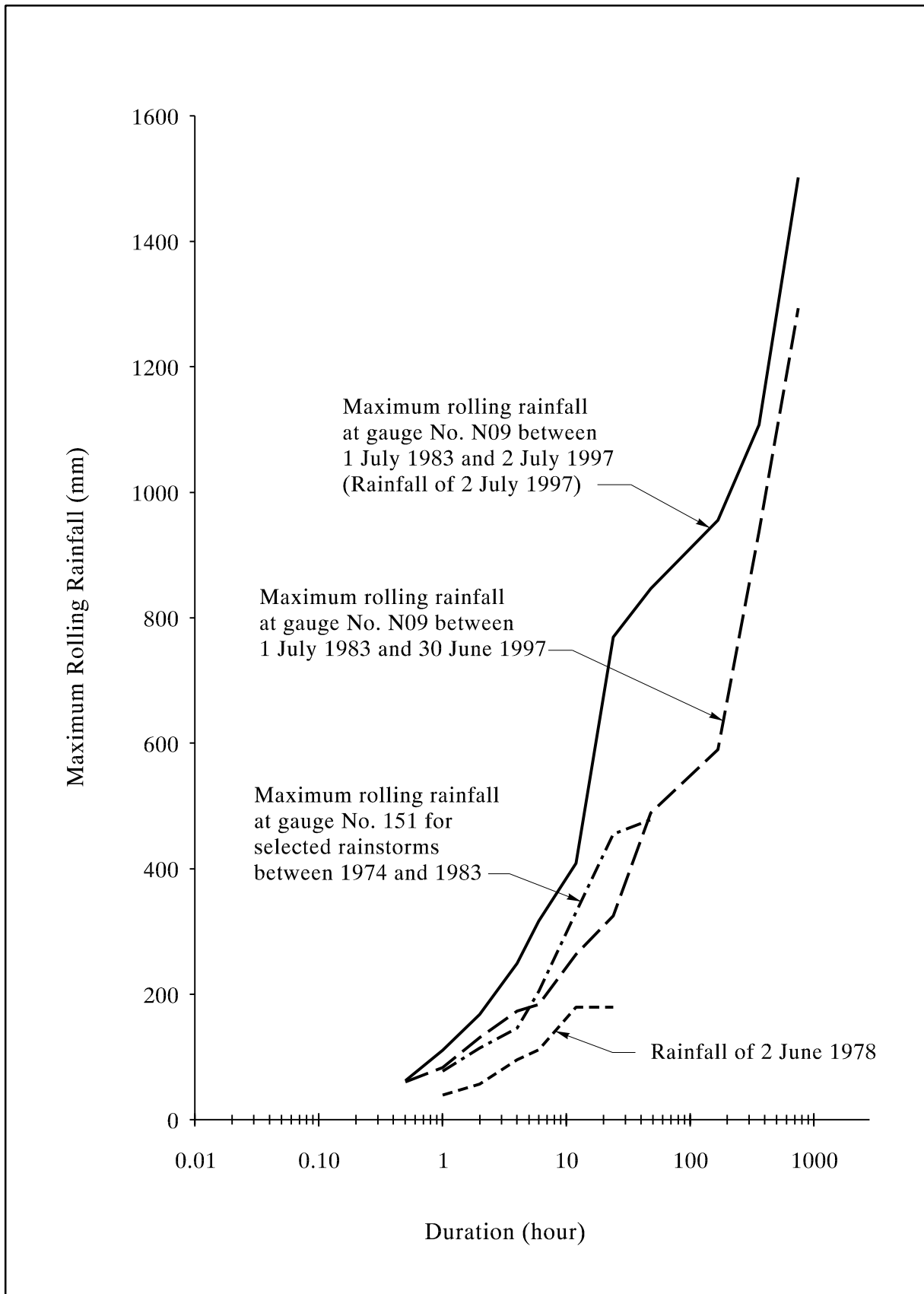


Figure 19 - Maximum Rolling Rainfall at Raingauge No. N09 and at the Autographic Raingauge No. 151 at the Chinese University

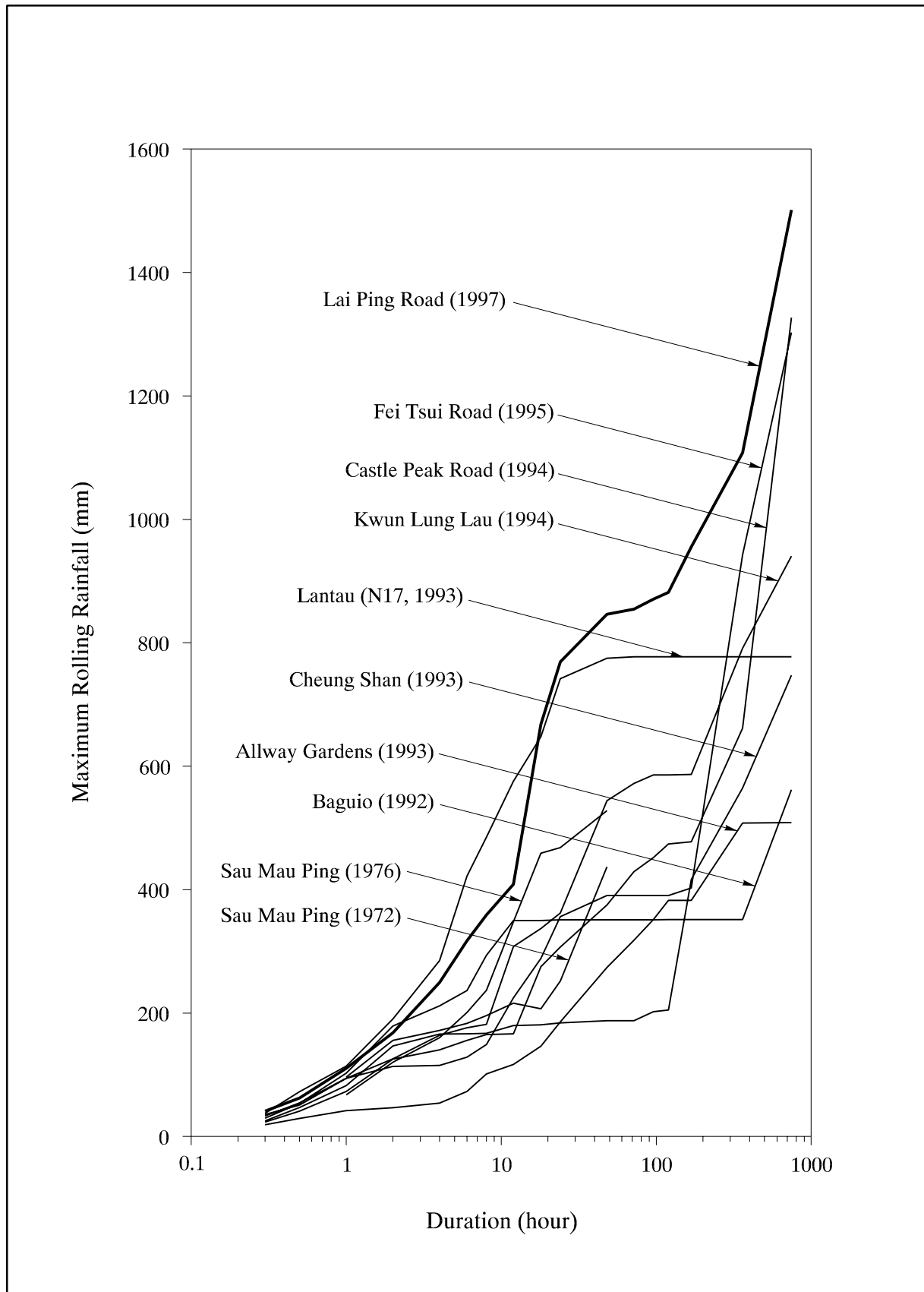


Figure 20 - Comparison of Rainfall Data Recorded at Raingauge No. N09 with Other Raingauges for Major Landslide Events

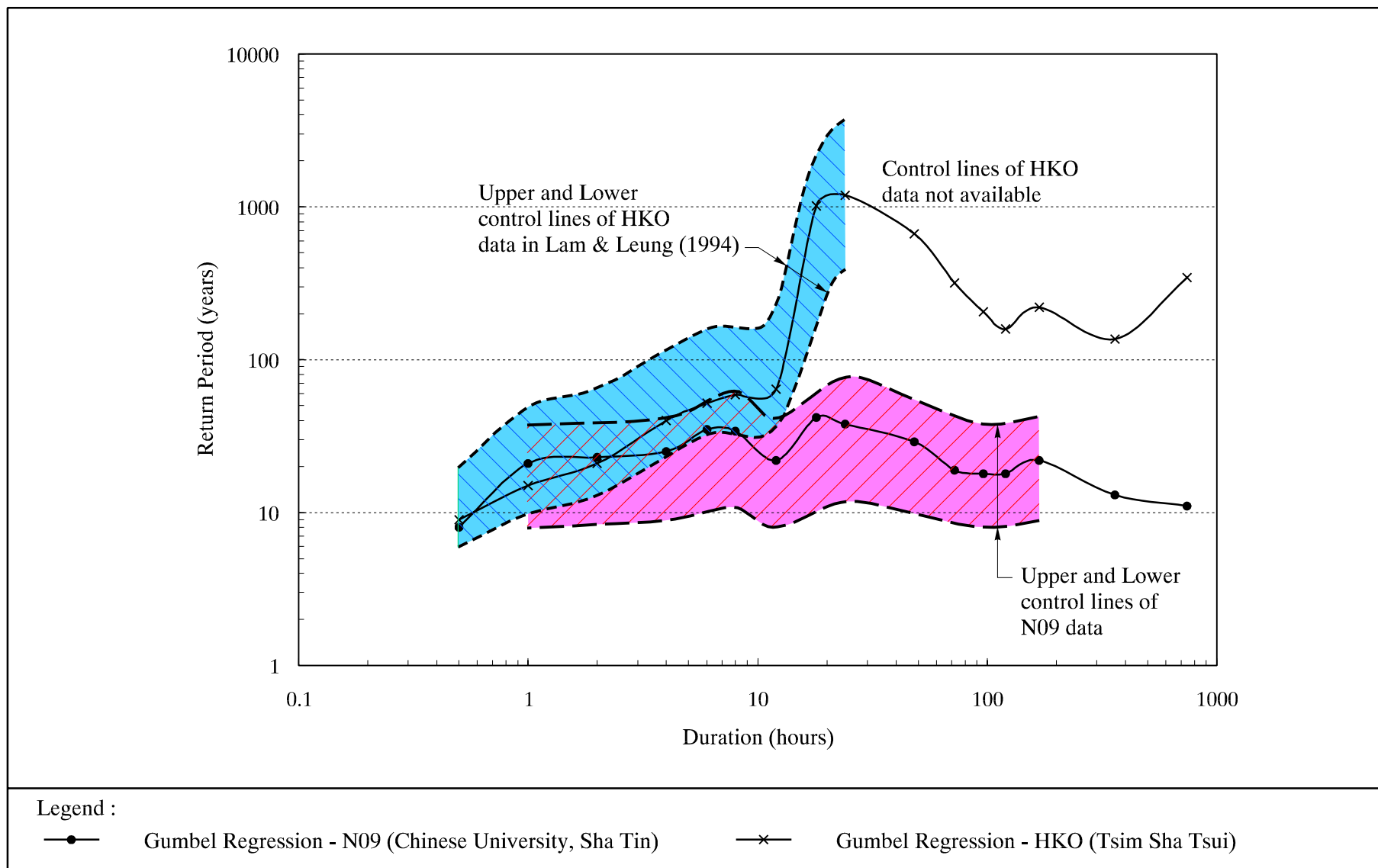
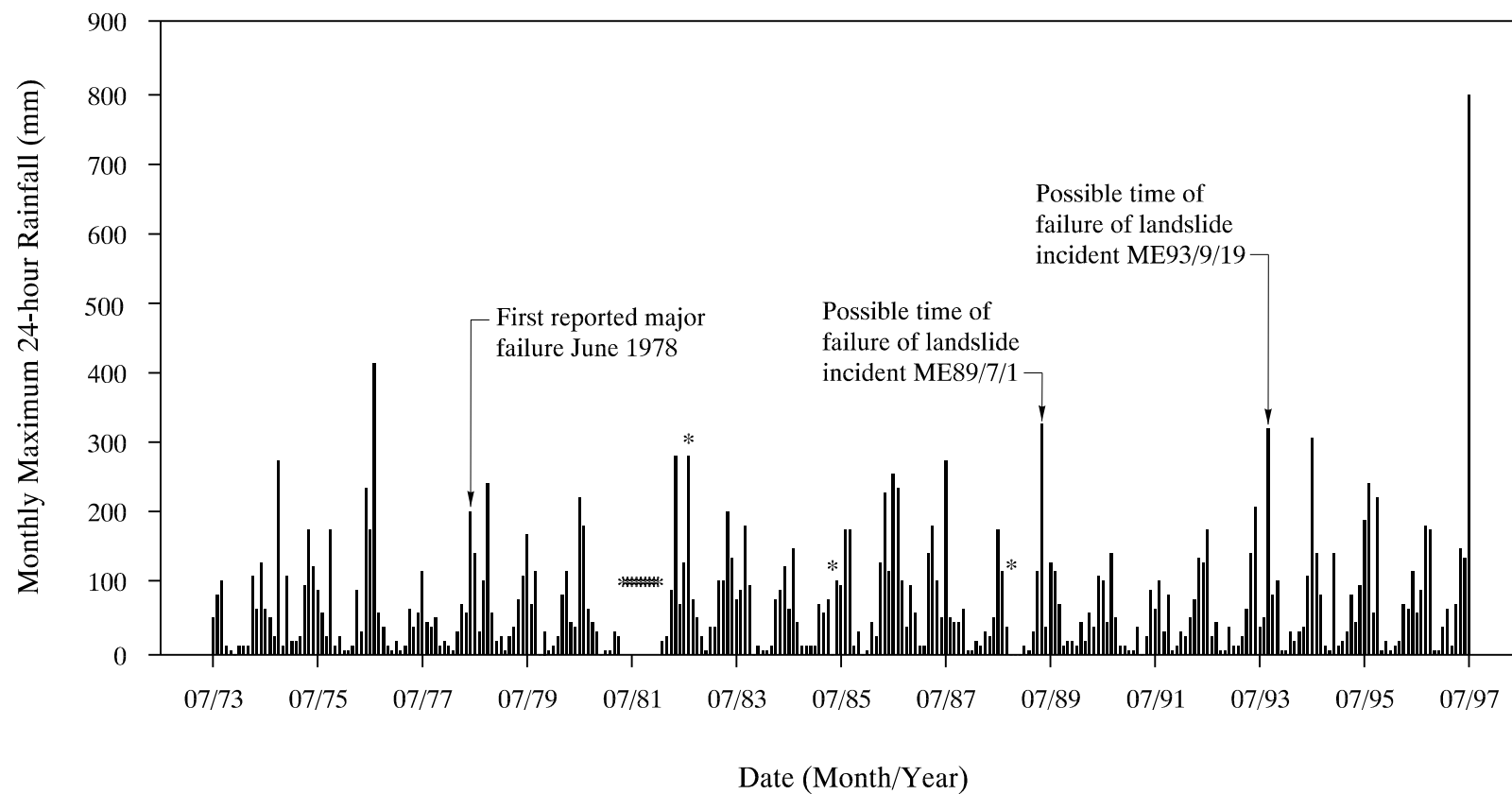


Figure 21 - Return Period of the Maximum Rainfall Recorded at Raingauge No. N09



Legend :

* Data incomplete

Note : July 73 - Dec 83 daily rainfall data of HKO Gauge No.151
Jan 84 - July 97 5-minute rainfall data of Gauge No.N09

Figure 22 - Monthly Maximum 24-hour Rainfall at the Chinese University Between July 1973 and July 1997

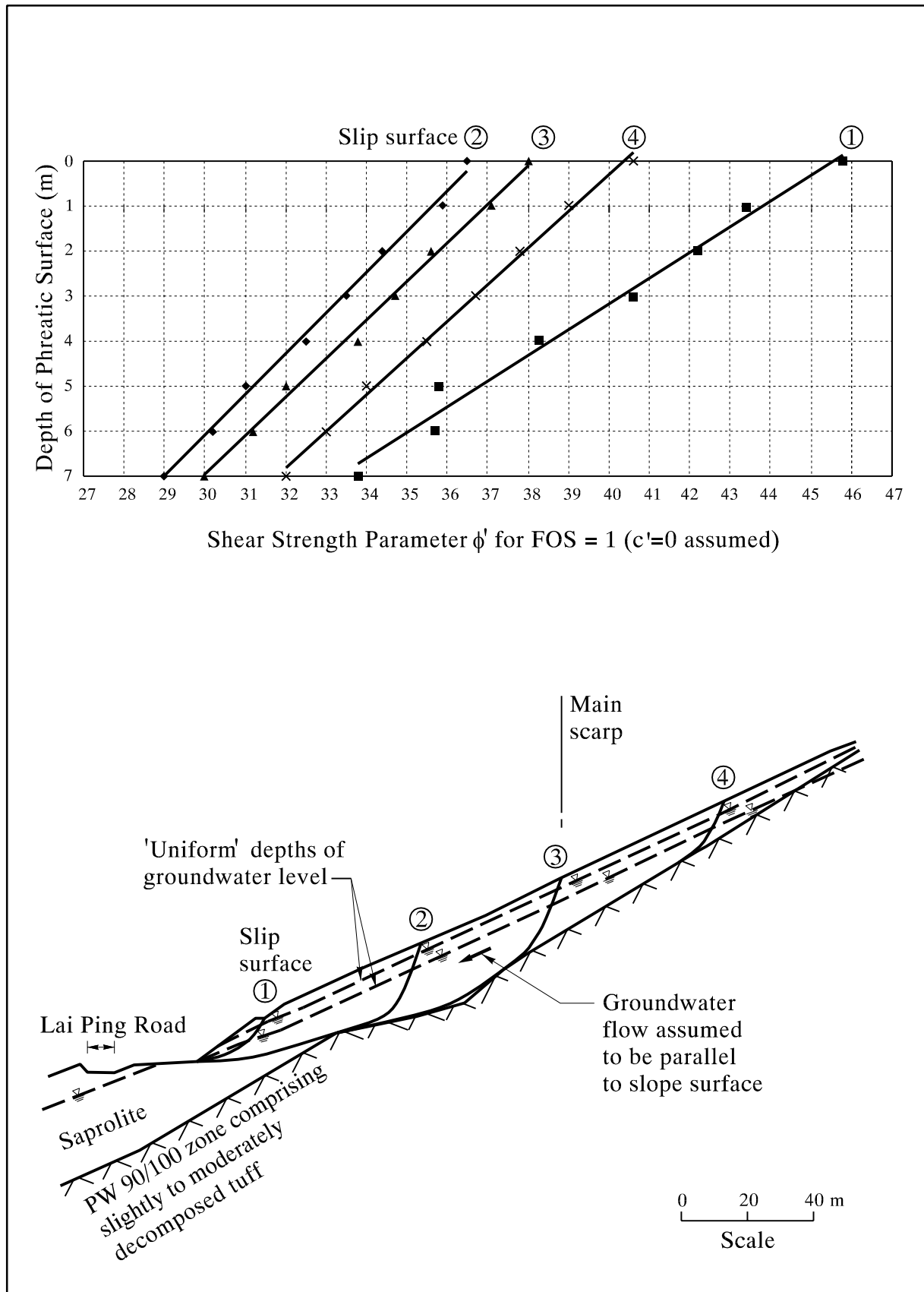


Figure 23 - Sensitivity of Shear Strength on Slip Surfaces and Depth of Groundwater Table on Slope Stability

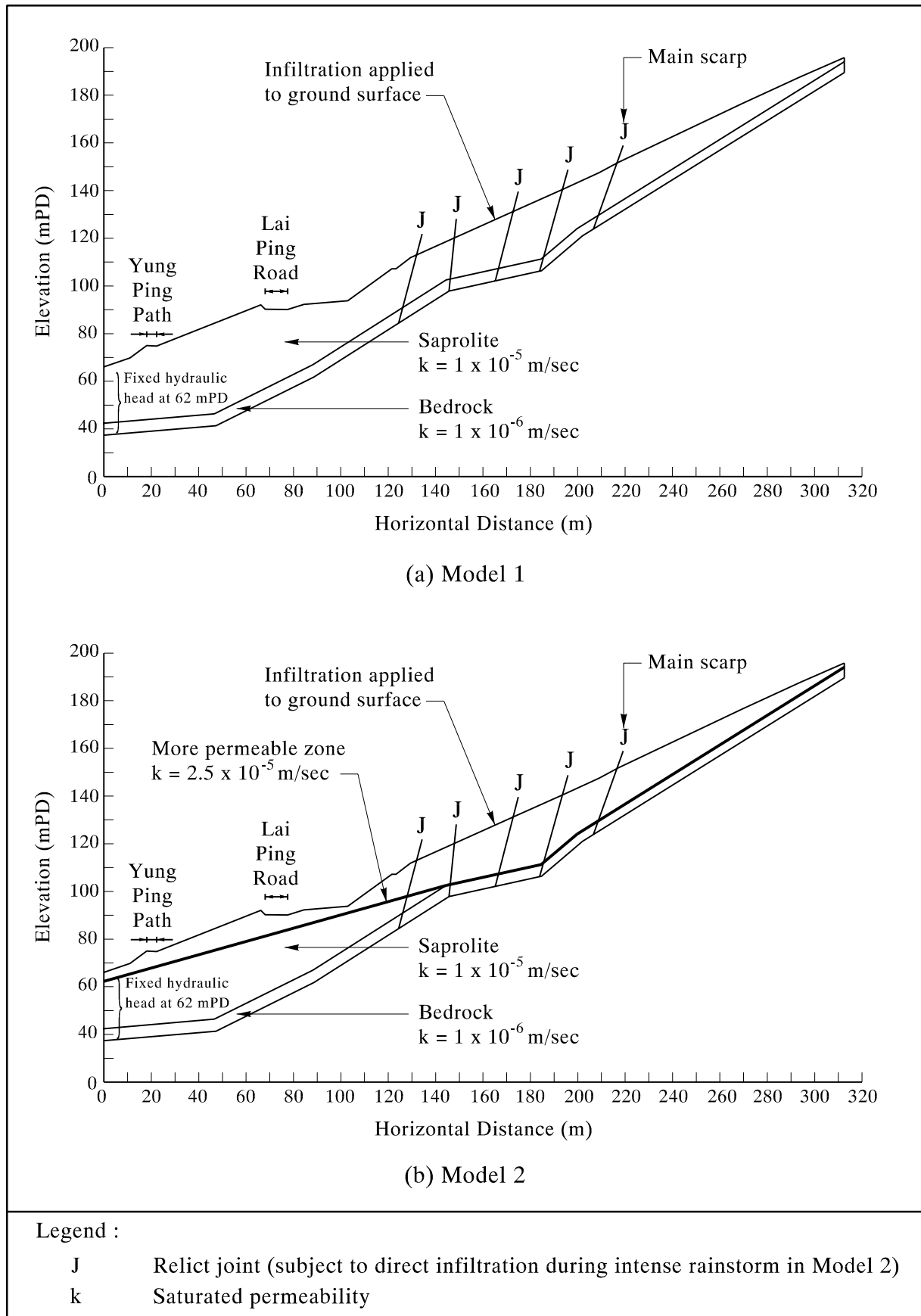


Figure 24 - Finite Element Mesh for Seepage Analyses

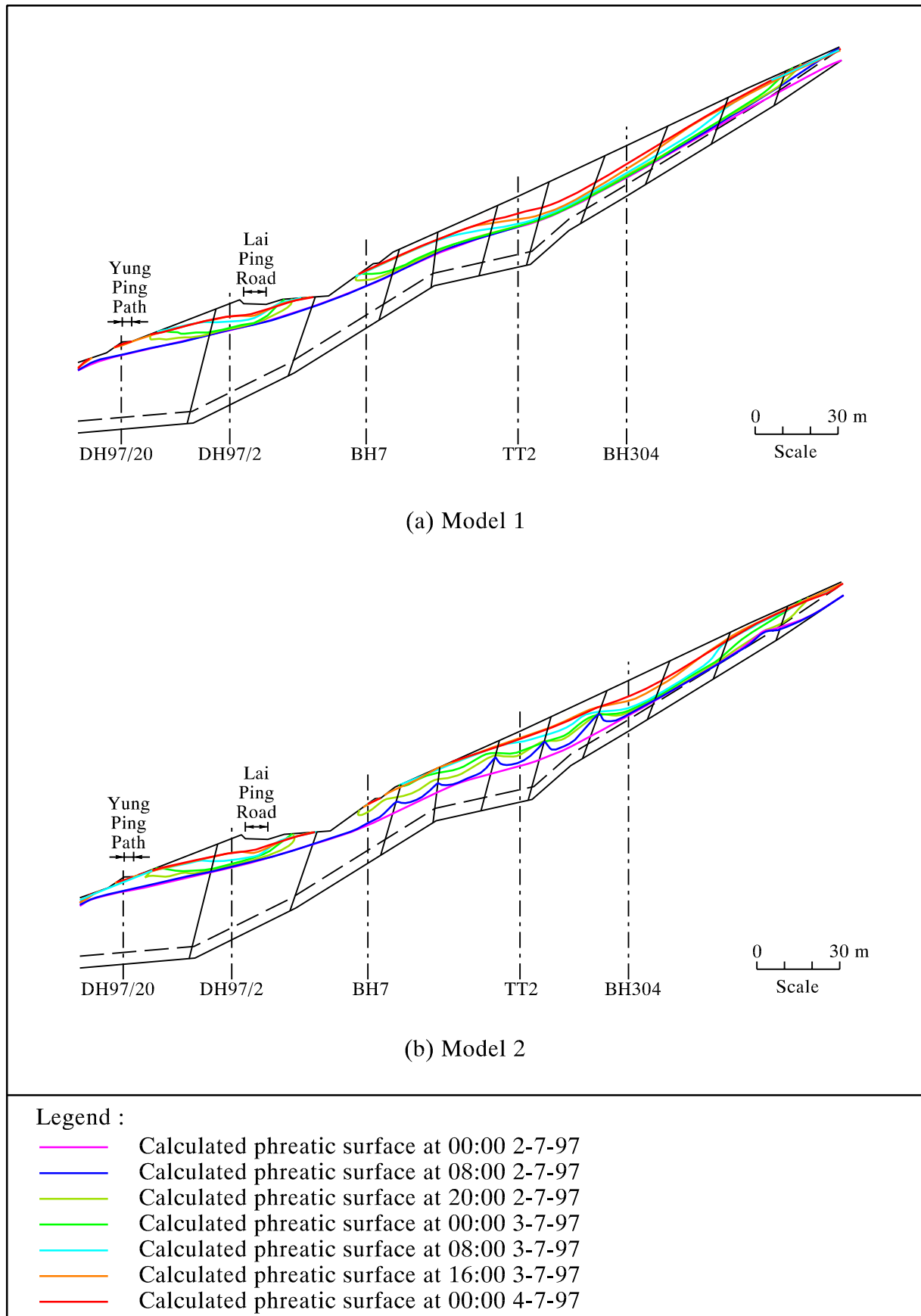


Figure 25 - Changes of Phreatic Surface Calculated by Seepage Analyses

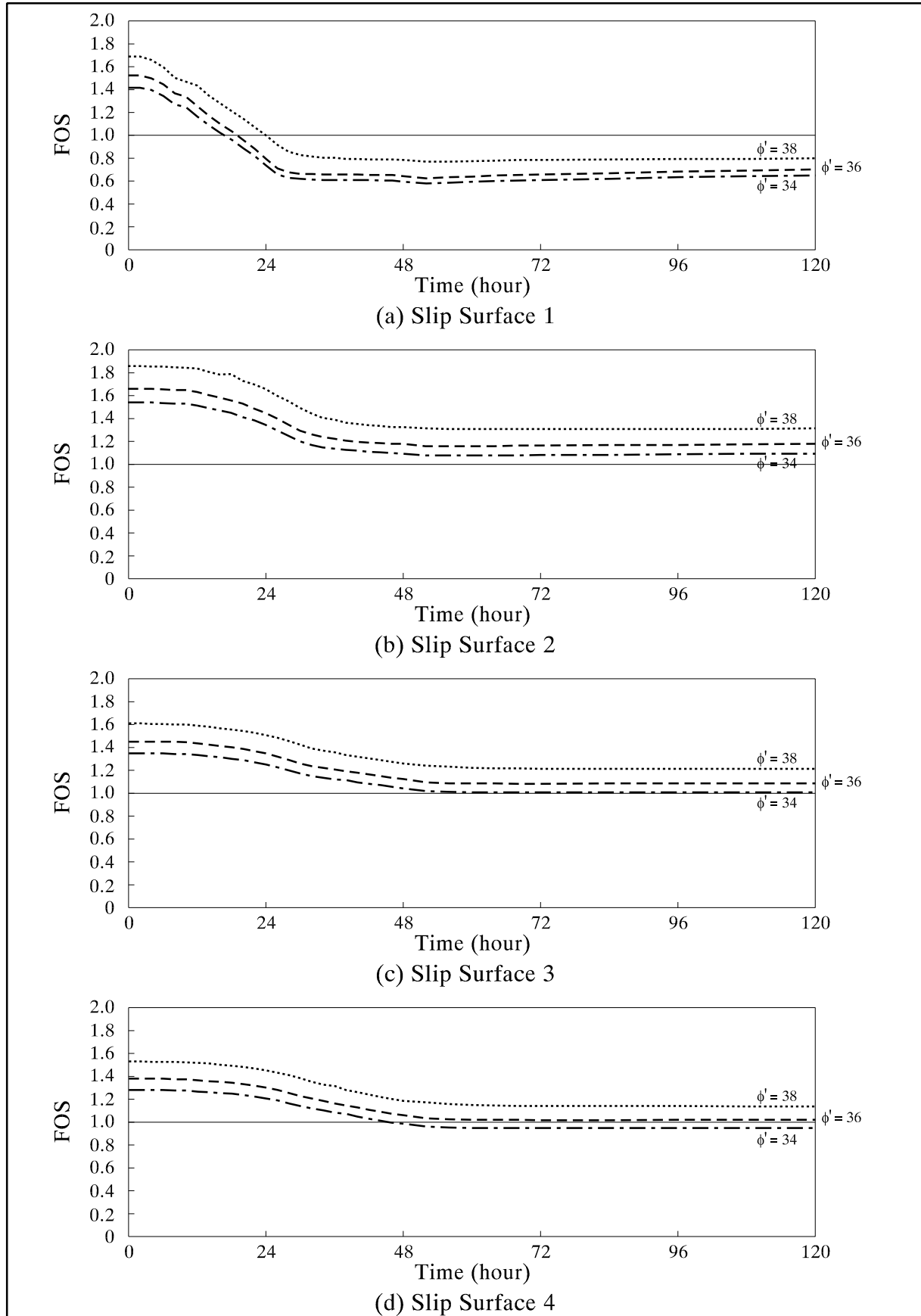


Figure 26 - Temporal Variation of Factor of Safety of Slip Surfaces 1 to 4 - Model 1

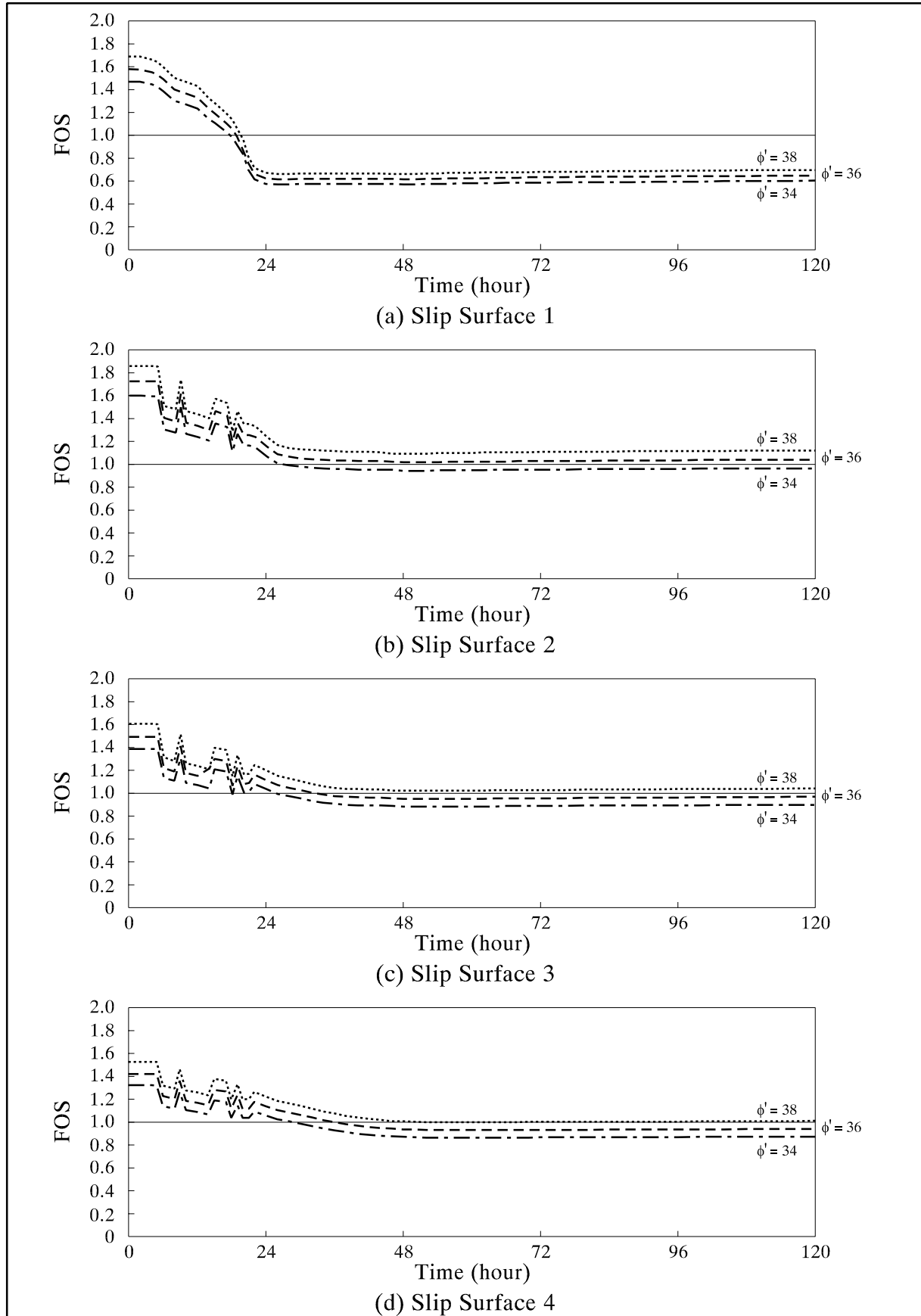


Figure 27 - Temporal Variation of Factor of Safety of Slip Surfaces 1 to 4 - Model 2

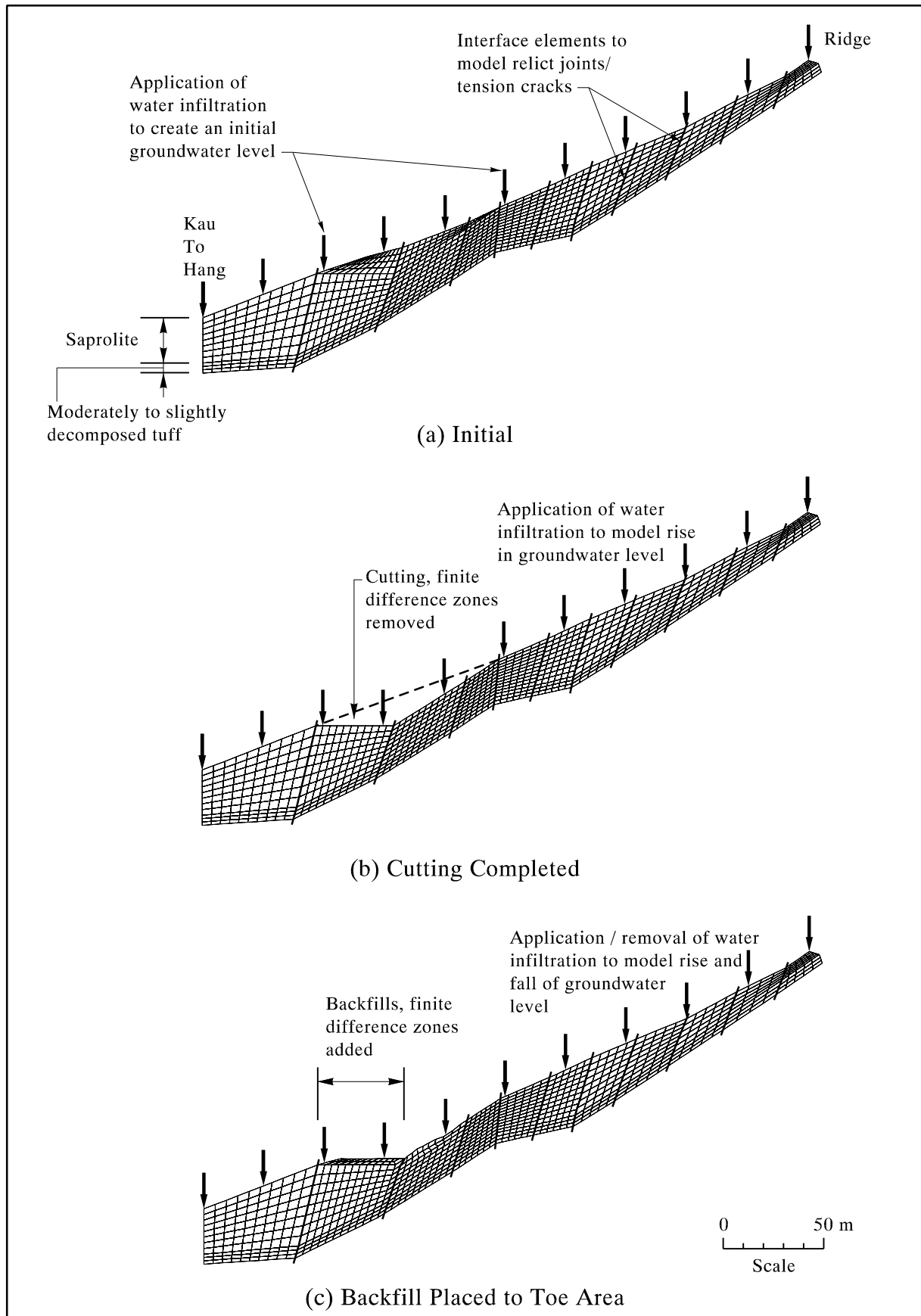


Figure 28 - Finite Difference Grid for Cross-Section 6-6'

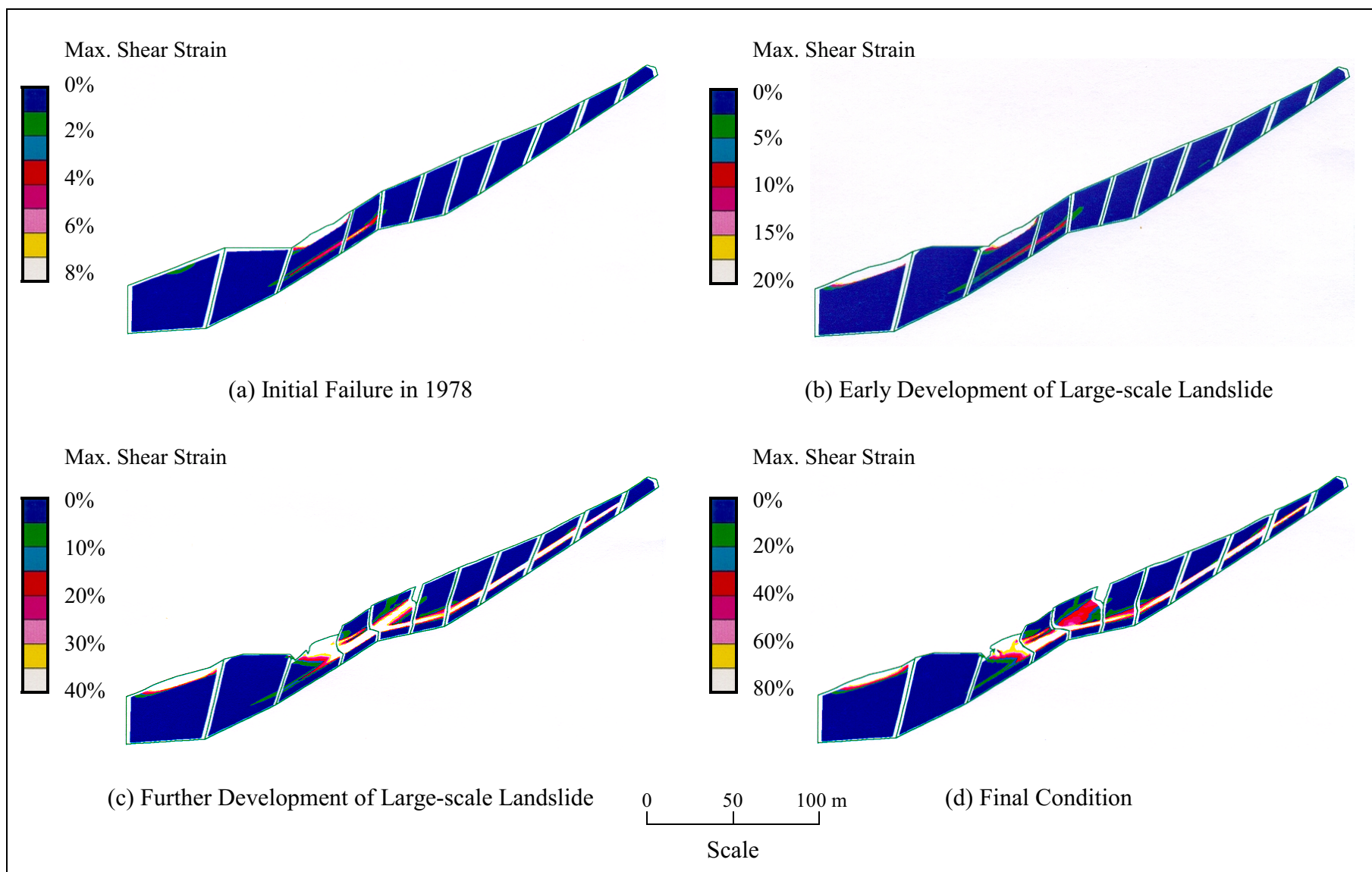


Figure 29 - Shear Strain Mobilisation During the Development of the Landslide Mechanism - Finite Difference Analysis

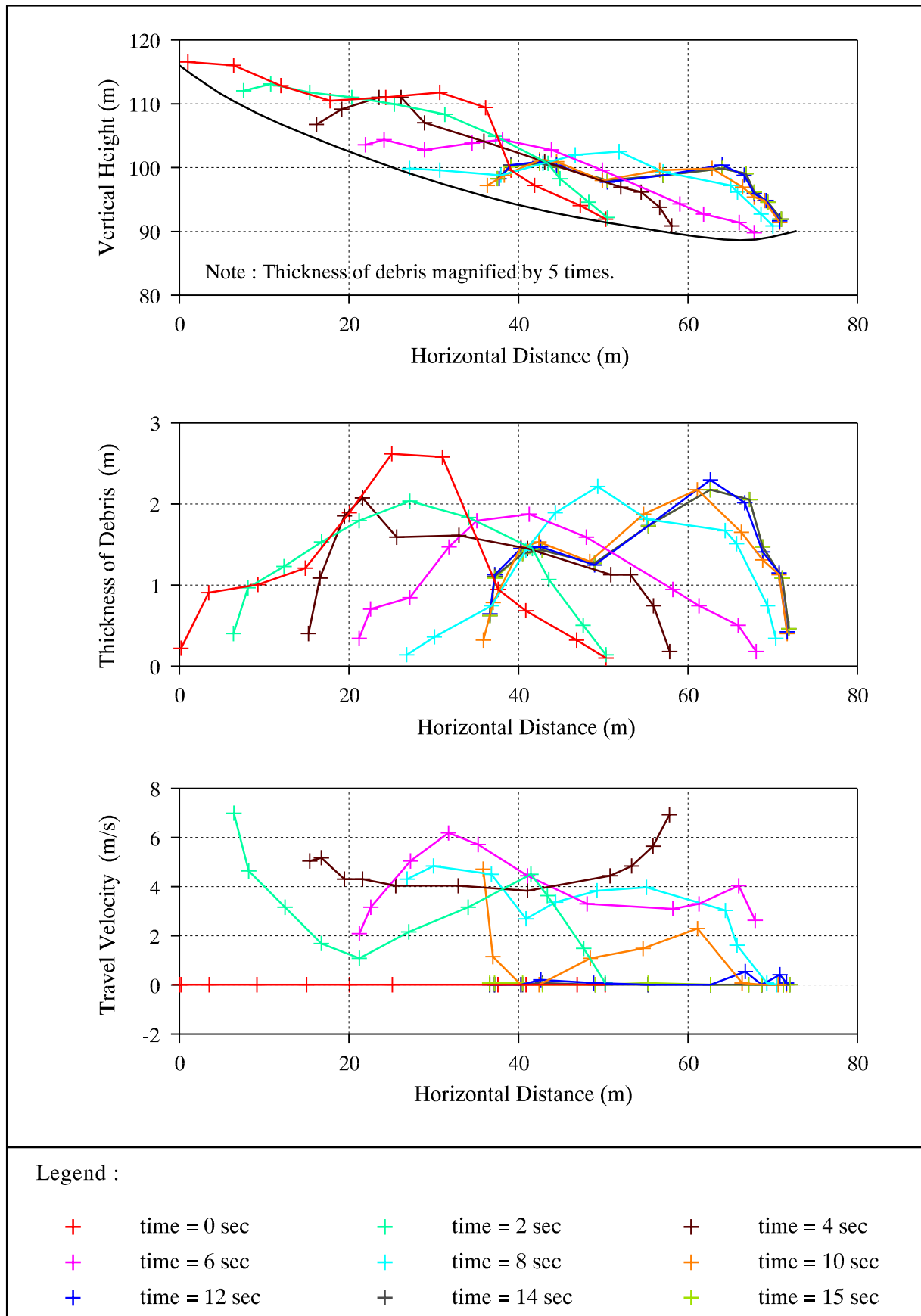


Figure 30 - Dynamic Analysis of Mobility of Landslide Debris from Scar No. 1

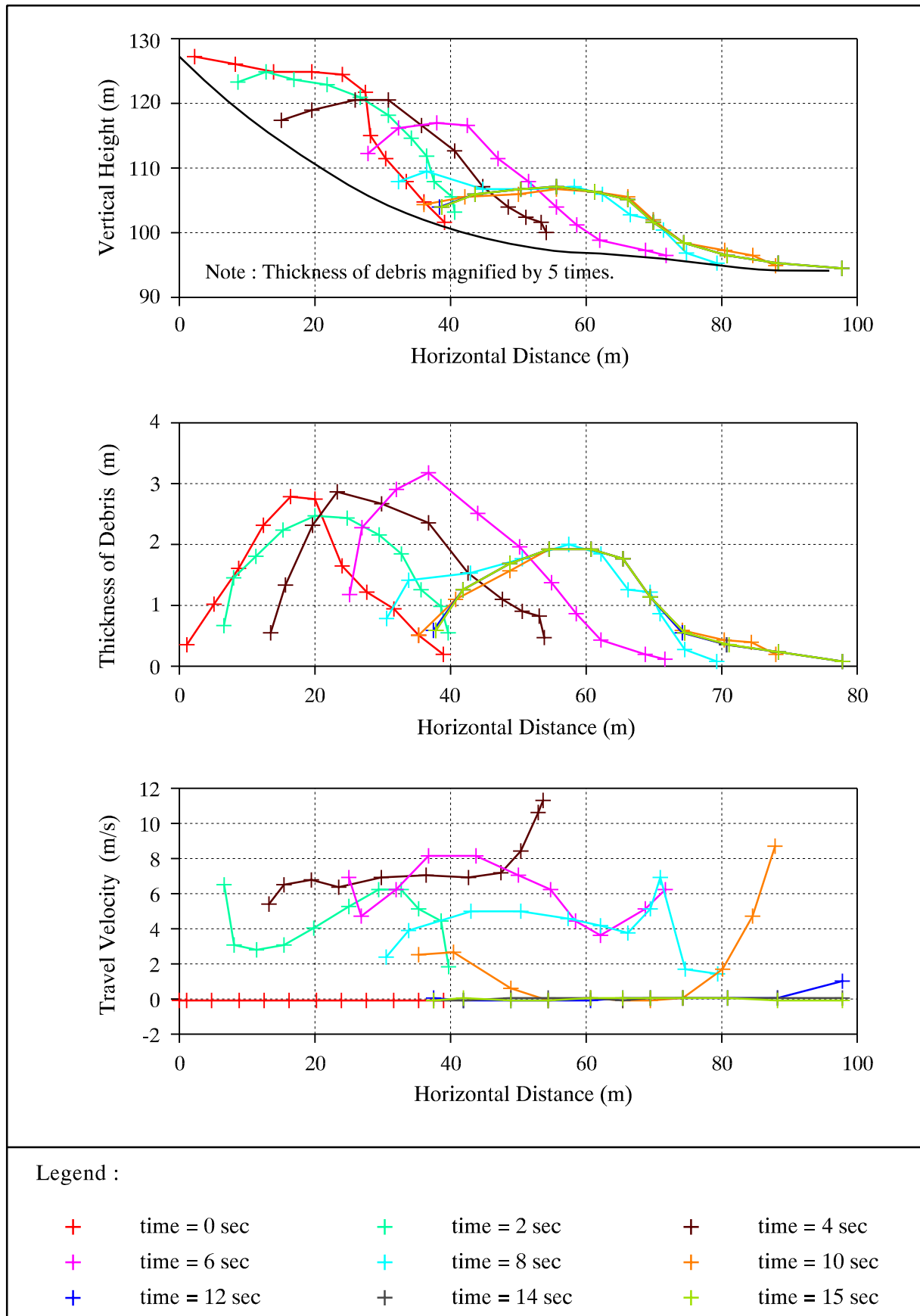


Figure 31 - Dynamic Analysis of Mobility of Landslide Debris from Scar No. 4